doi:10.1093/brain/awl359 *Brain* (2007), **130**, 630–653

Association fibre pathways of the brain: parallel observations from diffusion spectrum imaging and autoradiography

Jeremy D. Schmahmann,[1] Deepak N. Pandya,[3] Ruopeng Wang,[2] Guangping Dai,[2] Helen E. D'Arceuil,[2] Alex J. de Crespigny[2] and Van J. Wedeen[2]

[1]Department of Neurology, [2]Martinos Center for Biomedical Imaging, Department of Radiology, Massachusetts General Hospital and Harvard Medical School and [3]Department of Anatomy and Neurobiology, Boston University School of Medicine, Boston, MA, USA

Correspondence to: Jeremy D. Schmahmann, MD, Department of Neurology, Massachusetts General Hospital, CPZS-340, 55 Fruit Street, Boston MA 02114, USA
E-mail: jschmahmann@partners.org

Understanding the long association pathways that convey cortical connections is a critical step in exploring the anatomic substrates of cognition in health and disease. Diffusion tensor imaging (DTI) is able to demonstrate fibre tracts non-invasively, but present approaches have been hampered by the inability to visualize fibres that have intersecting trajectories (crossing fibres), and by the lack of a detailed map of the origins, course and terminations of the white matter pathways. We therefore used diffusion spectrum imaging (DSI) that has the ability to resolve crossing fibres at the scale of single MRI voxels, and identified the long association tracts in the monkey brain. We then compared the results with available expositions of white matter pathways in the monkey using autoradiographic histological tract tracing. We identified 10 long association fibre bundles with DSI that match the observations in the isotope material: emanating from the parietal lobe, the superior longitudinal fasciculus subcomponents I, II and III; from the occipital-parietal region, the fronto-occipital fasciculus; from the temporal lobe, the middle longitudinal fasciculus and from rostral to caudal, the uncinate fasciculus, extreme capsule and arcuate fasciculus; from the occipital-temporal region, the inferior longitudinal fasciculus; and from the cingulate gyrus, the cingulum bundle. We suggest new interpretations of the putative functions of these fibre bundles based on the cortical areas that they link. These findings using DSI and validated with reference to autoradiographic tract tracing in the monkey represent a considerable advance in the understanding of the fibre pathways in the cerebral white matter. By replicating the major features of these tracts identified by histological techniques in monkey, we show that DSI has the potential to cast new light on the organization of the human brain in the normal state and in clinical disorders.

Keywords: tract tracing; tractography; fibre bundles; diffusion tensor imaging; isotope; disconnection

Abbreviations: AF = arcuate fasciculus; ASs = superior limb of the arcuate sulcus; CB = cingulum bundle; CC = corpus callosum; CS = central sulcus; DSI = diffusion spectrum imaging; DTI = diffusion tensor imaging; DWI = diffusion weighted image; EmC = extreme capsule; EPI = echoplanar imaging; FOF = fronto-occipital fasciculus; ILF = inferior longitudinal fasciculus; IPS = intraparietal sulcus; L In = limen insulae; MB = subcallosal fasciculus of Muratoff; MdLF = middle longitudinal fasciculus; RS = rostral sulcus; SLF = superior longitudinal fasciculus; SMA = supplementary motor area (M II); STS = superior temporal sulcus; UF = uncinate fasciculus

Received October 20, 2006. Revised November 21, 2006. Accepted November 28, 2006. Advance Access publication February 9, 2007

Introduction

Disconnection syndromes from white matter lesions have long been recognized (Wernicke, 1874; Dejerine, 1892; Liepmann and Maas, 1907), and close attention to this entity by Geschwind (1965) revitalized the field of behavioural neurology. Evidence is now mounting that abnormalities of the cerebral white matter detected on magnetic resonance imaging (MRI) are associated with cognitive decline in the ageing brain (e.g. Peters *et al.*, 1994; Gunning-Dixon and Raz, 2000; Peters, 2002), and that

white matter diseases result in overt dementia (e.g. Filley, 2001; Au *et al.*, 2006; Schmahmann and Pandya, 2006). There is, therefore, a pressing need to define the anatomy and connections of the cerebral white matter tracts in order to understand the relational architecture, and hence the function, of the large-scale neurocognitive networks that subserve cognitive functions (Mesulam, foreword in Schmahmann and Pandya, 2006).

There is presently no histological method available to study the trajectory of the association pathways in the human brain. Recent technical and conceptual developments in MRI using diffusion tensor imaging (DTI) and diffusion tractography have made it possible to visualize association fibre pathways *in vivo* (e.g. Basser *et al.*, 1994, 2000; Makris *et al.*, 1997; Catani *et al.*, 2002; Mori and van Zijl, 2002). There are, however, two intractable shortcomings inherent in the DTI studies to date.

First, there are technical limitations with the DTI approach itself, related in large part to the probability that a given voxel contains a substantial number of fibres with intersecting trajectories (crossing fibres). Present MRI methods based on diffusion contrast have been developed to map fibre orientations in tissue, and from these orientations to infer large-scale fibre geometries. The first of these methods, DTI, suffers a fundamental drawback in that the millimetre resolution characteristic of MRI results in partial volume averaging. As a result, mixing of different fibre populations occurs within a single resolved image location (voxel), and the diffusion tensor may provide ambiguous and/or inaccurate descriptions of local fibre orientations. Accurate mapping of fibre architecture in the central nervous system using DTI may, therefore, be open to question in any region of complex fibre architecture, particularly where the trajectories of different fibres intersect. These DTI problems with partial volume averaging and the ubiquitous nature of fibre crossing can be addressed using diffusion spectrum imaging (DSI), an essentially model-free imaging approach that has the ability to map complex fibre architecture at the scale of single MRI voxels (Tuch *et al.*, 2002; Wedeen *et al.*, 2005; Wedeen VJ, Wang RP, Schmahmann JD, Benner T, Tseng WYI, D'Arcuiel H *et al.* submitted for publication). It is this method that we employ in the present study to decipher the organization of the major cerebral association fibre tracts.

The second problem with the present DTI studies is the inability to validate the findings with reference to a comprehensive anatomical exposition of the detailed trajectory of the cerebral white matter architecture. In order to conclude that MRI of the white matter tracts is accurate, the mathematical models that are interpreted by the sophisticated imaging tools must reflect the known anatomy. But the 'known' anatomy of the tracts in the human is not as established as the current literature suggests. Validation of the DTI observations in the human brain to date has relied upon findings from pioneering investigators who used gross dissection, myelin stains and lesion degeneration methods in human clinical cases for fibre tract identification (e.g. Reil, 1809; Burdach, 1822–26; Meynert, 1885; Dejerine, 1895). These approaches resulted in inaccuracies and terminological confusion, attested to by intense debates in the early literature (e.g. Schröder, 1901; see also Schmahmann and Pandya, 2006). Moreover, these early human studies could not provide information regarding the origins and terminations of the association tracts.

A solution to this conundrum has been advanced by the autoradiographic tract tracing study of the white matter of the rhesus monkey brain (Schmahmann and Pandya, 2006). This comprehensive analysis provides a detailed map of the trajectory of the different fibre pathways. It should now be possible to compare the results of MR tractography in the monkey with the knowledge of these tracts that has been established with accepted histological techniques. A compelling and clinically motivated reason to study white matter tracts in the monkey with both the autoradiographic and the MRI approaches is that if the DSI methodology is validated, it may then be applied to the human brain in health and disease.

In this study, therefore, we investigated the cerebral association pathways in the monkey using the DSI methodology in order to take advantage of the available knowledge regarding the long association pathways identified in monkey using experimental tract tracing.

Material and methods

Isotope technique

The histological observations described in this study were obtained from the brains of rhesus monkeys as described in Schmahmann and Pandya (2006). Material was prepared using the autoradiographic technique according to Cowan *et al.* (1972). Data were analysed under dark-field microscopy (Fig. 1) and the pathways were analysed and portrayed on external views of the surface of the cerebral hemisphere. As details of these fibre pathways using the isotope technique have recently been published, here we present only brief descriptions derived from that study in order to compare them with the novel DSI data.

DSI material preparation

We used the brains of four adult male fascicularis monkeys (8–10 kg) that were part of a study of stroke in primates. After euthanasia, brains were perfused, fixed with formalin, removed from the cranium and further immersion fixed in formalin for at least 4 weeks. Brains were then soaked for at least 28 days in a buffer solution containing gadolinium (Gd-DTPA) MRI contrast agent to reduce the T_1 relaxation time, and scanned on a 4.7 T Bruker Biospec system. Brains used in this study were from a group with small transient ischaemic lesions that were not visible on the DSI scans. Cortical association fibres were studied in the contralesional hemisphere in which abnormalities would not be expected.

DSI methodology

The pulse sequence was a 3D diffusion weighted spin-echo echo-planar imaging (EPI) sequence, TR/TE 450/63 ms, with an imaging matrix of $172 \times 86 \times 128$ pixels with isotropic spatial resolution of

$512\,\mu m^3$. Diffusion spectrum encoding was performed as previously described (Wedeen *et al.*, 2005). It consisted of 515 diffusion weighted measurements, corresponding to a cubic lattice in Q-space contained within the interior of a ball of maximum radius $b_{max} = 4 \times 10^4\,cm^2\,s^{-1}$, with $\delta = 12$ ms, $\Delta = 31$ ms. Total acquisition time was 25 h. Diffusion spectra were reconstructed for each voxel by 3D Fourier transform of the modulus of the acquired data. Orientation vectors of maximum diffusion were identified at each voxel, and every such vector used to initiate a fibre trajectory. Trajectories were propagated by Euler integration always pursuing the orientation vector of least curvature, halting where this curvature exceeded a threshold of 0.5 radians (35°) per voxel. The complete data set for each monkey specimen consisted of 1.5 million such fibre solutions (Fig. 2). Trajectories were displayed on a 3D workstation with interactive software developed by our laboratory (TrackVis, Wedeen *et al.* manuscript in review).

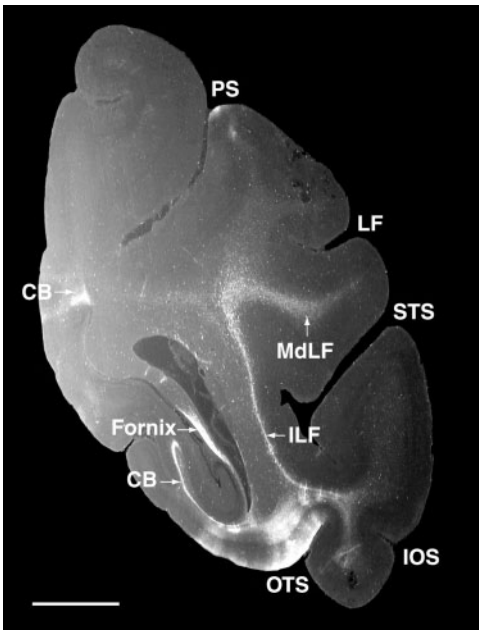

Fig. 1 Representative low power dark field photomicrograph of a coronal section through the cerebral hemisphere of a rhesus monkey shows labelled fibres coursing through the cerebral white matter to their termination sites. These fibres were identified with autoradiography following injection of isotope labelled amino acids into the parahippocampal gyrus, area TF. Long association fibres in the dorsal and ventral limbs of the CB, the MdLF and the ILF are seen, as well as fibres coursing in the fornix to the dorsal hippocampal commissure (bar = 5 mm). See list of abbreviations. Fig. 1 reproduced from Schmahmann and Pandya, 2006.

DSI data analysis

Localization of fibre bundles was performed using specialized software tools developed for this purpose. Regions are determined within which the fibre bundles are expected to be present, based on the location and trajectory of the fibre pathways as determined by the isotope study. Within this volume the precise bundle of interest is identified as a set of fibres intersecting a small disc with a particular orientation. This differs from the approach adopted with DTI tractography that generally defines two ROIs, identifies all the fibres within each, and determines which fibres are common to both (e.g. Catani *et al.*, 2005). In DSI the ROI is substantially larger (about 40%) than the bundles that it contains. The disc placed over the data set has a particular orientation, and the fibres that traverse the disc do so also with a particular orientation (Fig. 3). We exclude short fibres, so that the fibres intersecting the disc are long fibres conforming to the trajectory of the expected bundle. By using a liberal definition of the ROI the subset of fibres intersecting the disc that emerges from the larger data set constitutes the bundle in question. Unlike DTI therefore, with DSI a single ROI is adequate for the task. This is a central aspect of DSI, and an advantage of the method. The anatomic trajectory of each individual bundle is defined by displaying its intersection with 2D slices and 3D rendered surfaces of the brain in multiple views. The 2D views, projected into the same data volume as the fibres, are extracted from the low *b*-value (grey matter bright, white matter darker) or average high *b*-value (white matter bright, grey matter dark) diffusion-weighted EPI volumes of the same brain. These are displayed as slices through the data, and the degree of transparency and 3D viewing angle are all under

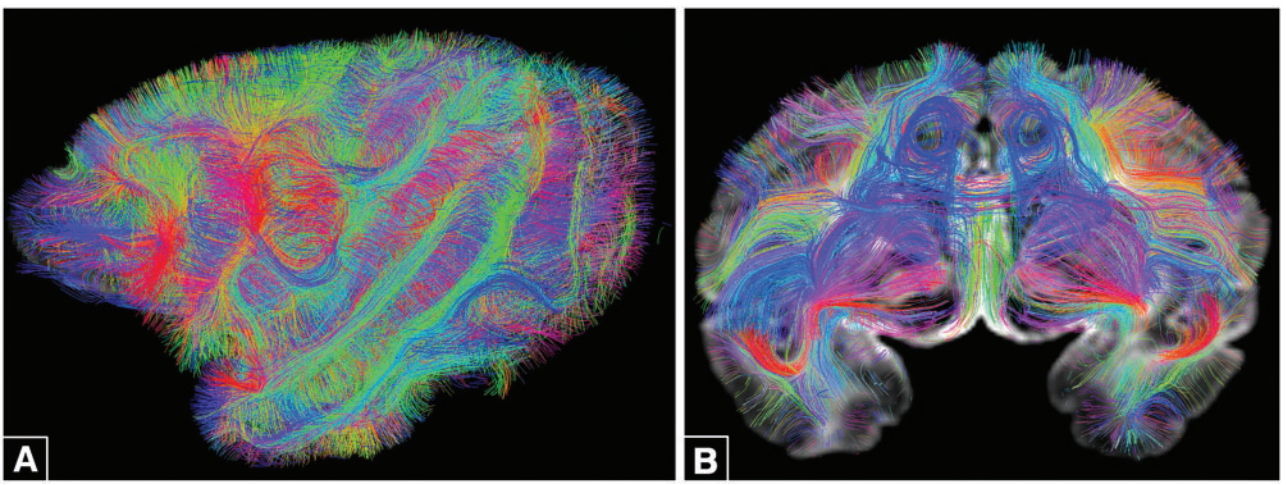

Fig. 2 Representative views derived from the DSI data set of a monkey brain. (**A**) Lateral view of 10% of the 1.5 million fibre solutions. (**B**) Fibres incident upon a coronal cross section through the data. Each fibre is shown with a constant colour according to the orientation vector between its end-points.

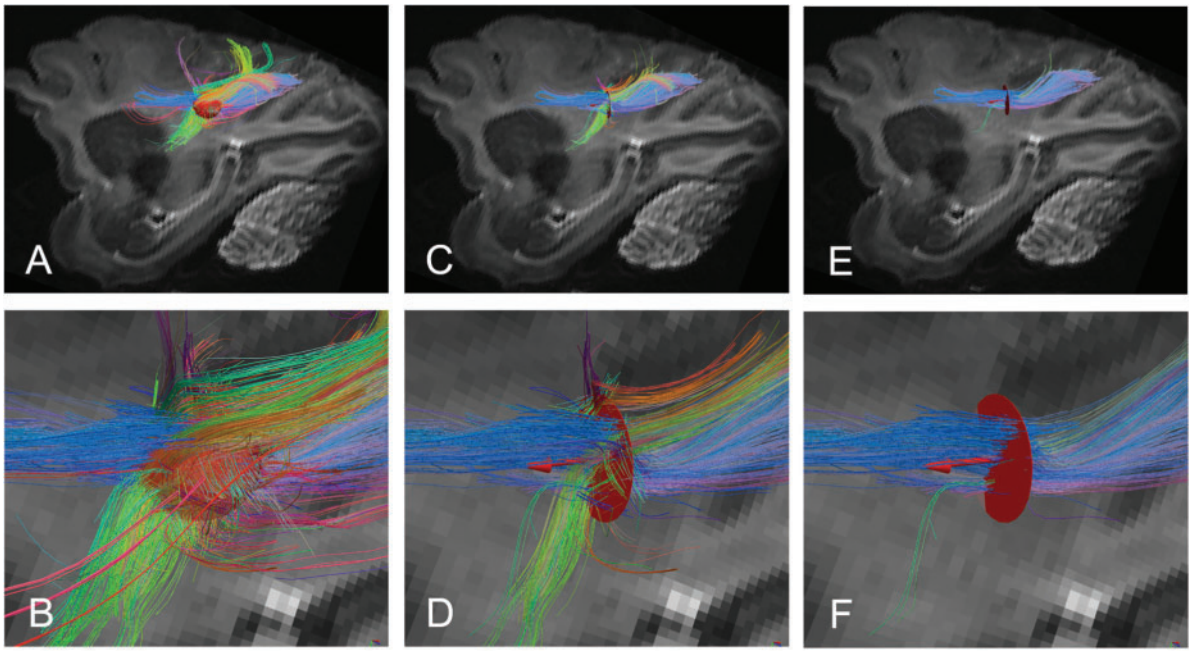

Fig. 3 Identification of fibre bundles with DSI tractography using a single region of interest (ROI)—example of SLF III. **A**, **C** and **E** are low power views, and **B**, **D** and **F** are magnified views of these images, respectively. **A** and **B** show a spherical ROI placed in the parietal lobe white matter, and the fibres that intersect the sphere including the SLF III plus many non-SLF III fibres. **C** and **D** show a disc of the same radius as the sphere in **A** and **B**, with a particular orientation identified by the red arrow. The disc now intersects a much reduced set of non-SLF III fibres. **E** and **F** show the disc with the orientation identified by the red arrow, intersecting only those fibres that cross the disk at angles $<30^{\circ}$. This image shows few if any stray fibres, and the fibres identified comprise the set we have defined as SLF III.

interactive control. This process is guided by the fibre trajectories identified by the isotope method. Multiple fibre bundles are displayed simultaneously to confirm their spatial relationships. The colour-coding of fibres is based on standard RGB code applied to the vector between the end-points of each fibre. Blue indicates the rostrocaudal direction; red the mediolateral plane; and green the dorsoventral orientation.

Results

The association fibre pathways emerging from the different sectors of the cerebral hemisphere are described, first from the data obtained with the autoradiographic method, and then according to DSI.

The long association pathways of the cerebral white matter are grouped here by cortical area of origin. For parietal lobe, the superior longitudinal fasciculus (SLF) I, II and III; for occipital-parietal region, the fronto-occipital fasciculus (FOF); for temporal lobe, the middle longitudinal fasciculus (MdLF) and from rostral to caudal, the uncinate fasciculus (UF), extreme capsule (EmC) and arcuate fasciculus (AF); for occipital-temporal region, the inferior longitudinal fasciculus (ILF); and for the cingulate gyrus, the cingulum bundle (CB). The connections conveyed by all these fasciculi are bidirectional, and whereas the direction of the association fibres can be ascertained by the isotope study from the location of the injection of the anterograde tracer, DSI cannot discern whether the association fibres are entering or emanating from a given cortical area.

Parietal lobe

The SLF and AF have historically been regarded as a single fibre bundle in the human (Reil, 1809; Burdach, 1822–26; Dejerine, 1895). Isotope studies in the monkey (Petrides and Pandya, 1984; Schmahmann and Pandya, 2006) indicate, however, that the SLF itself is not a single fibre tract, and that it is separate from the arcuate fascicle that arises from the temporal lobe. These isotope investigations as well as DTI analyses in human (Makris *et al.*, 2005) reveal that the SLF can be divided into three dorsal to ventral components in the white matter of the parietal and frontal lobes – SLF I, II and III. The FOF also conveys fibres between the parietal and the frontal lobes.

Superior longitudinal fasciculus, subcomponent I (SLF I)

Isotope. The autoradiographic material reveals that the SLF I fibre bundle courses in the white matter of the superior parietal and superior frontal lobules (Fig. 4B). It lies dorsal to and distinct from the CB. It extends from the medial and dorsal parietal cortex to the dorsal part of the premotor and prefrontal cortices (Fig. 4A). The SLF I links medial parietal areas PEc, PGm, 31, and superior parietal lobule area PE, with dorsal area 6, dorsal area 9,

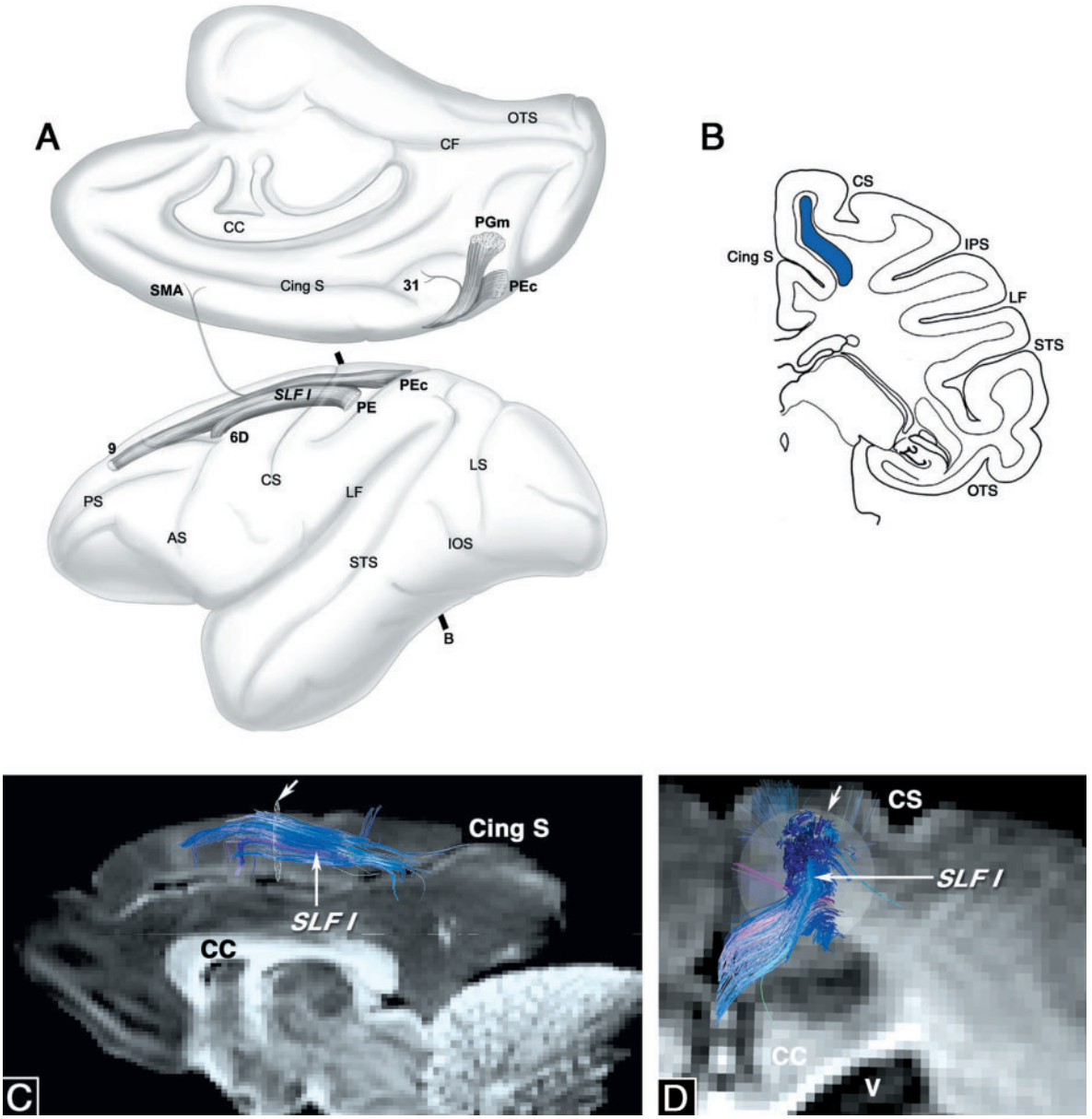

Fig. 4 Diagrams depicting the SLF I. **A** and **B** are illustrations derived from the autoradiographic tract tracing study; **C** and **D** show the fibres detected in the DSI study. (**A**) Surface views of the medial (top) and lateral convexities (lower) of the monkey cerebral hemisphere show the trajectory of the SLF I reflected onto the cortical surface, and the cortical areas that it links. (**B**) Coronal section taken at the level demarcated in **A** shows the location of the SLF I (shaded in blue) in the white matter of the superior frontal gyrus. (**C**) Sagittal depiction of the trajectory of the SLF I fibres that intersect the disc (arrow) superimposed upon a diffusion weighted image (DWI) of a medial view of the cerebral hemisphere. (**D**) Partial view of a coronal image of the dorsal part of the cerebral hemisphere shows the rostrocaudally directed fibres in the SLF I intersecting the disc (white grid) in the white matter of the superior frontal gyrus. The DWI represents a single coronal slice, whereas the entire SLF I fascicle is seen end-on. Fibres are seen coursing rostral to the disc as well as caudal to it. See list of abbreviations. Fig. 4 (A) reproduced from Schmahmann and Pandya, 2006.

and the supplementary motor area (SMA) in the frontal lobe (Fig. 4A).

DSI. When the disc is placed within the white matter of the superior frontal gyrus, a group of fibres is seen running in the rostral–caudal dimension that occupies a similar location to the SLF I identified in the isotope material. This is shown both on the sagittal orientation (Fig. 4C) and in the coronal view (Fig. 4D). The fibre bundle occupies almost the entire dorsal–ventral dimension of the white matter of the superior parietal and frontal gyri, also in agreement with the findings of the isotope material. The fibres within this bundle reach the posterior parietal region, area PEc laterally and areas PGm and 31 medially. In the frontal lobe, the fibres course towards the SMA and medial premotor region.

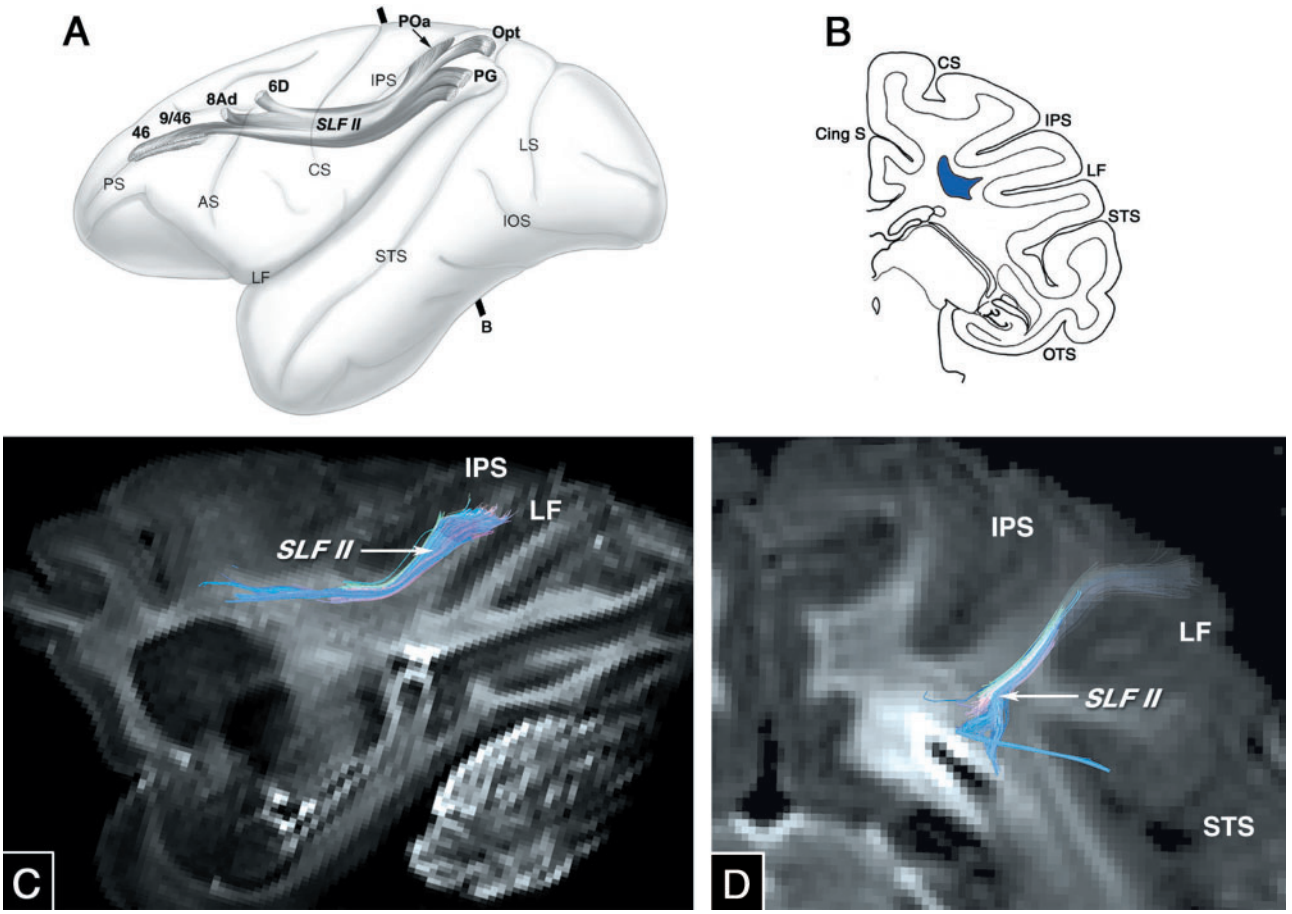

Fig. 5 Diagrams depicting the SLF II as determined by the isotope (**A, B**) and DSI techniques (**C, D**). (**A**) Surface view of the lateral convexity of the cerebral hemisphere of the rhesus monkey shows the trajectory of the SLF II reflected onto the cortical surface, and the cortical areas that it links. (**B**) Coronal section through a hemisphere of the monkey brain taken at the level demarcated in A shows the location of the SLF II fibre bundle (blue filled area). (**C**) SLF II fibres are shown in the sagittal plane superimposed upon a DWI view of the cerebral hemisphere. (**D**) End-on depiction of fibres in the location of the SLF II superimposed upon a partial view of a DWI coronal section of the cerebral hemisphere. See list of abbreviations. Fig. 5 (A) reproduced from Schmahmann and Pandya, 2006.

Superior longitudinal fasciculus, subcomponent II (SLF II)

Isotope. The autoradiographic study shows that SLF II stretches from the caudal part of the inferior parietal lobule to the dorsal premotor and prefrontal cortices (Fig. 5A). It lies caudally within the white matter of the inferior parietal lobule, then deep to the upper shoulder of the sylvian fissure (Fig. 5B). More rostrally it extends into the white matter beneath the premotor and prefrontal regions. This SLF II interlinks area POa in the intraparietal sulcus (IPS), and areas PG and Opt of the inferior parietal lobule with areas 46, 9/46, 8Ad and 6D in the frontal lobe.

DSI. The placement of the sphere in the inferior parietal lobule results in the definition of fibres travelling between the posterior parietal region and the frontal lobe (Fig. 5C). The fibres that lie first within the white matter of the inferior parietal lobule are consistent in course and destination with the SLF II long association bundle identified by the isotope tract tracing, coursing rostrally in the centrum semiovale (Fig. 5D). Fibres peel off from the main SLF II bundle heading towards destinations in the caudal prefrontal cortex (regions corresponding to dorsal areas 6, 8 and 46).

Superior longitudinal fasciculus, subcomponent III (SLF III)

Isotope. In the tract tracing study the SLF III fibre bundle is identified in the opercular white matter of the parietal and frontal lobes, extending from the rostral inferior parietal lobule to the ventral part of the premotor and prefrontal cortex (Fig. 6A and B). The SLF III links area POa in the IPS, and areas PF, PFG and PFop of the parietal lobe, and ventral premotor area 6, 44 and ventral prefrontal area 9/46 v of the frontal lobe.

DSI. The sphere placed over a rostral and ventral location within the inferior parietal lobule identifies the SLF III. These fibres course in a broad plate occupying the white matter of the parietal and frontal opercula, with a trajectory towards the ventral part of the frontal lobe (Fig. 6C–E). Fibres leave the SLF III in the frontal lobe in a location

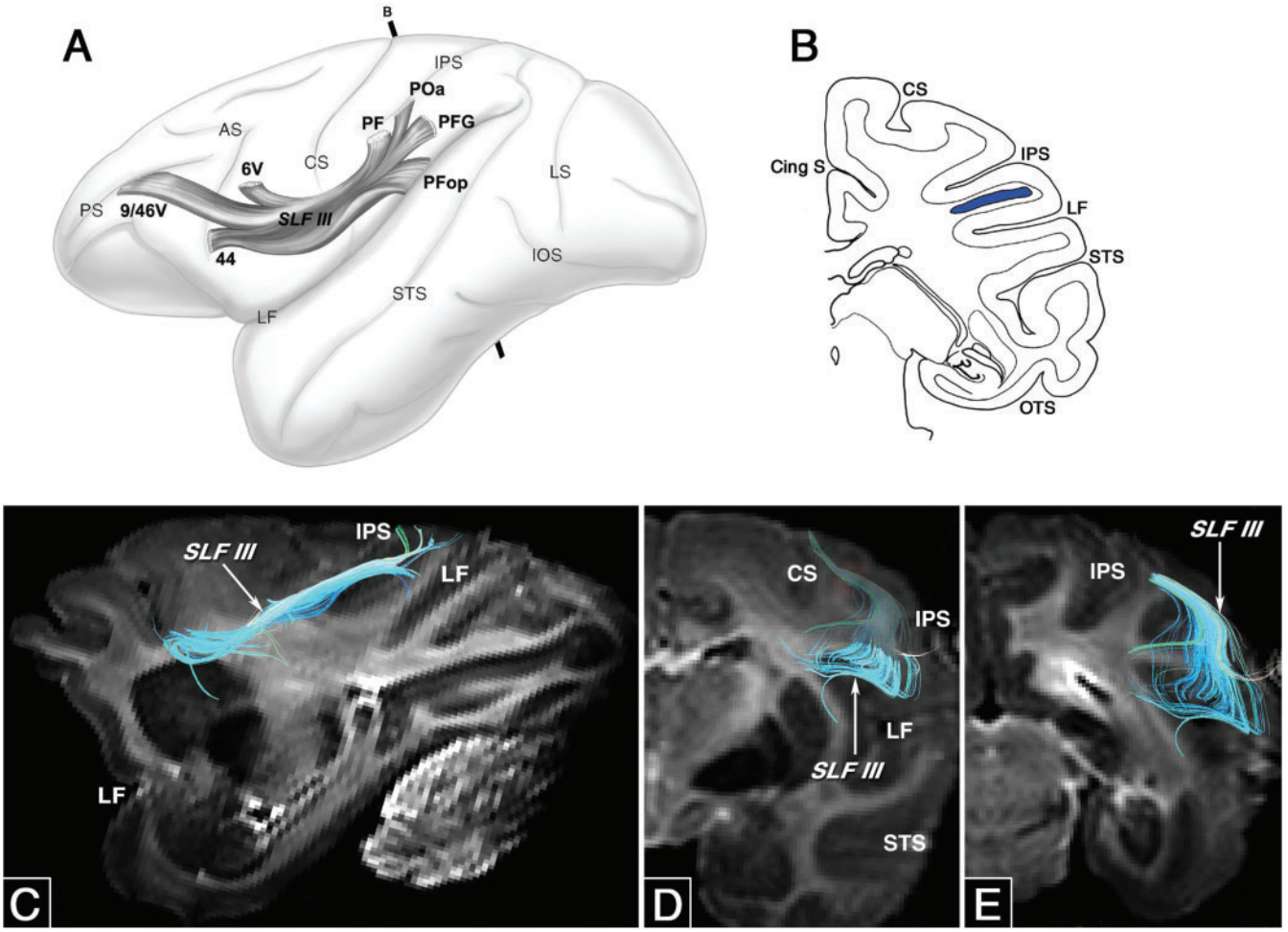

Fig. 6 Diagrams depicting the SLF III as determined by the isotope (**A, B**) and DSI techniques (**C–E**). (**A**) Surface view of the lateral convexity of the cerebral hemisphere of the rhesus monkey shows the trajectory of the SLF III reflected onto the cortical surface, and the cortical areas that it links. (**B**) Coronal section through a hemisphere of the monkey brain taken at the level demarcated in **A** to show the location of the SLF III fibre bundle (blue filled area) in the white matter of the inferior parietal lobule. (**C**) SLF III fibres are shown in the rostral caudal dimension superimposed upon a DWI sagittal view of the cerebral hemisphere. (**D**) End-on view of fibres in the location of the SLF III coursing in the rostral–caudal direction seen with reference to a coronal section of the cerebral hemisphere taken through the parietal-frontal opercular white matter, and in **E** the fibres are seen against a more caudal rostral coronal DWI image coursing in the parietal lobe. See list of abbreviations. Fig. 6 (A) reproduced from Schmahmann and Pandya, 2006.

corresponding to the ventral premotor cortex area 6 V and area 44, as well as in prefrontal cortex area 9/46 v. The course and cortical destinations of this bundle are thus quite similar to those seen in the isotope case.

In order to compare the relative location and extent of the three components of the SLF, Fig. 7 shows the SLF I, II and III displayed together on the same sagittal and coronal views to better appreciate their distinct anatomical features.

Fronto-occipital fasciculus (FOF)

Isotope. The existence and location of the FOF were the subject of contentious debate in the historical literature (Schmahmann and Pandya, 2006), but the fibre bundle is readily identifiable in the experimental material. In the coronal plane it is triangular shaped and lies in the white matter above the caudate nucleus (Fig. 8B), superiorly abutting the shell of cortico caudate fibres closely adjacent to the caudate nucleus that constitutes the subcallosal fasciculus of Muratoff (Muratoff bundle, MB). The lateral boundary of the FOF is the corona radiata and the rostro-caudally oriented fibres of the SLF II, and medial to the FOF is the corpus callosum (CC). The fibres that form the FOF coalesce at a level just anterior to the atrium of the lateral ventricle, and course horizontally remaining above the MB until the frontal horn of the lateral ventricle. The FOF links the dorsal and medial parietal and occipital areas, i.e. areas PO, PGm, Opt, DP and PG, as well as caudal area 23, with frontal lobe areas 6D, 8Ad, 8B, 9 and 46d (Fig. 8A).

DSI. Following the placement of the disc in the white matter immediately above the body of the caudate nucleus

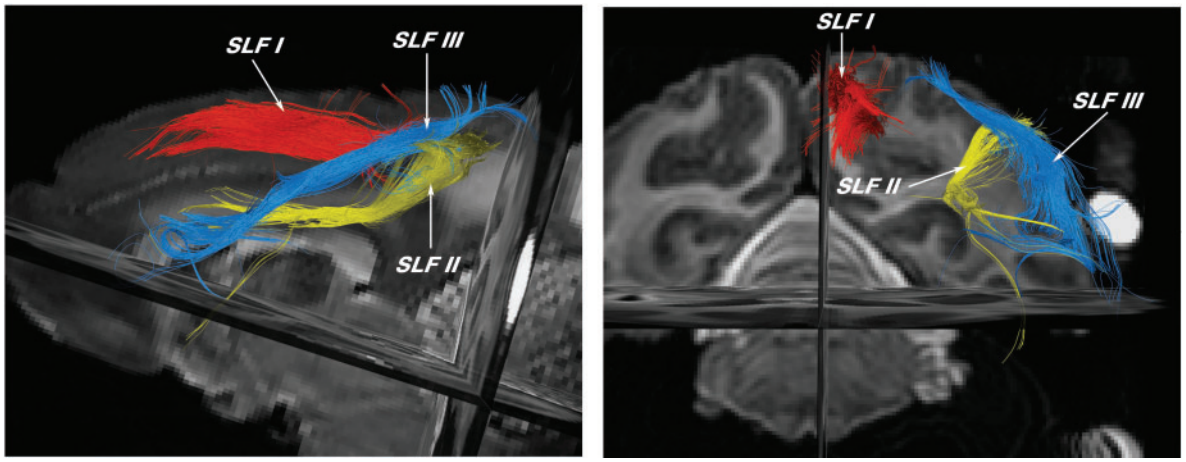

Fig. 7 Composite view showing the three subdivisions of the SLF seen with respect to the sagittal, horizontal and coronal planes of the cerebral hemisphere derived from DWI images. (**A**) Sagittal view; (**B**) Coronal view. Colour coding—SLF I red; SLF II yellow; SLF III blue.

two sets of horizontally running fibres are discernible (Fig. 8C). In the coronal plane (Fig. 8D and E) the FOF is the more dorsal of the two bundles, conforms roughly to a triangular shape, and has the appearance of loosely arranged bristles of a brush. At higher magnification (Fig. 8F), the dispersed fascicles that give rise to the bristled appearance of the FOF reflect the trajectory of fibre fascicles as they penetrate between callosal fibres coursing in the horizontal plane, and corona radiata fibres in the vertical plane. The more ventrally located fascicle travels as a dense and compact aggregate of fibres located immediately above the body of the caudate nucleus, lying between the caudate nucleus and the FOF. These fibres correspond to the location and characteristics of the subcallosal fasciculus of Muratoff (Fig. 8D–F). The two fibre bundles are observed also in the sagittal plane (Fig. 8C). The FOF extends from the parieto-occipital junction caudally to the dorsal prefrontal cortex rostrally, in general agreement with the detailed observations of the isotope study. The fibres in the MB that course rostral to the position of the disc stream down in multiple fibre fascicles into the striatum (Fig. 8C and E).

Temporal lobe

The long association fibre tracts in the temporal lobe are, from rostral to caudal, the UF, the EmC and the AF, as well as the MdLF that courses in the white matter of the superior temporal gyrus.

Uncinate fasciculus (UF)

Isotope. The UF is the most rostral temporal lobe fibre bundle. It courses between the rostral temporal cortices and the ventral, medial and orbital parts of the frontal lobe (Fig. 9A). Fibres that arise in the temporal lobe ascend in the temporal stem and move medially through the limen insulae into the white matter of the orbital cortex and then rostrally and medially in the frontal lobe (Fig. 9A and B). There are three main rostral temporal lobe areas interconnected with the frontal lobe—area TS1 of the rostral superior temporal region and the temporal proisocortex; inferior temporal areas TEa, IPa and TE1 and ventromedial temporal areas TH, TL and TF of the parahippocampal gyrus, the entorhinal and perirhinal cortices, and the amygdala. The UF is related in the frontal lobe to orbital areas 10, 11, 47/12, 13, 14 and 25. On the lateral prefrontal cortex it arises or terminates in areas 10, 47/12, and on the medial surface in areas 32 and rostral area 24 (Fig. 9A).

DSI. The disc was positioned in the white matter of the temporal lobe to include fibres traversing the temporal stem. The trajectory of the UF is seen optimally in sagittal profile and in the coronal plane. In the sagittal plane (Fig. 9C) the UF hooks around the limen insulae (L In) to link the temporal pole and the ventral prefrontal cortex. Contingents of fibres enter or leave this bundle from cortices in the ventromedial, inferotemporal and lateral temporal regions. These are clearly seen in the coronal plane (Fig. 9D), where the arching fibres in the L In are also well demarcated. In addition, the continuation of the UF fibres into the orbital frontal cortex and the medial prefrontal cortex are readily identified.

Extreme capsule (EmC)

Isotope. The EmC interconnects the mid-portion of the superior temporal region with the mid-portion of the ventral and lateral parts of the prefrontal cortex (Fig. 10A). It is situated between the claustrum and the insula (Fig. 10C). In the frontal lobe the EmC fibres divide into a superior ramus that lies in the white matter of the inferior frontal lobe, and an inferior ramus that lies beneath the claustrum on the floor of the orbital cortex, laterally adjacent to the fibres of the UF (Fig. 10B). Regions within the temporal lobe that contribute fibres to the EmC include the rostral insular cortex, areas TS2, TS3 and paAlt of the superior temporal gyrus, areas IPa, TAa and TPO of

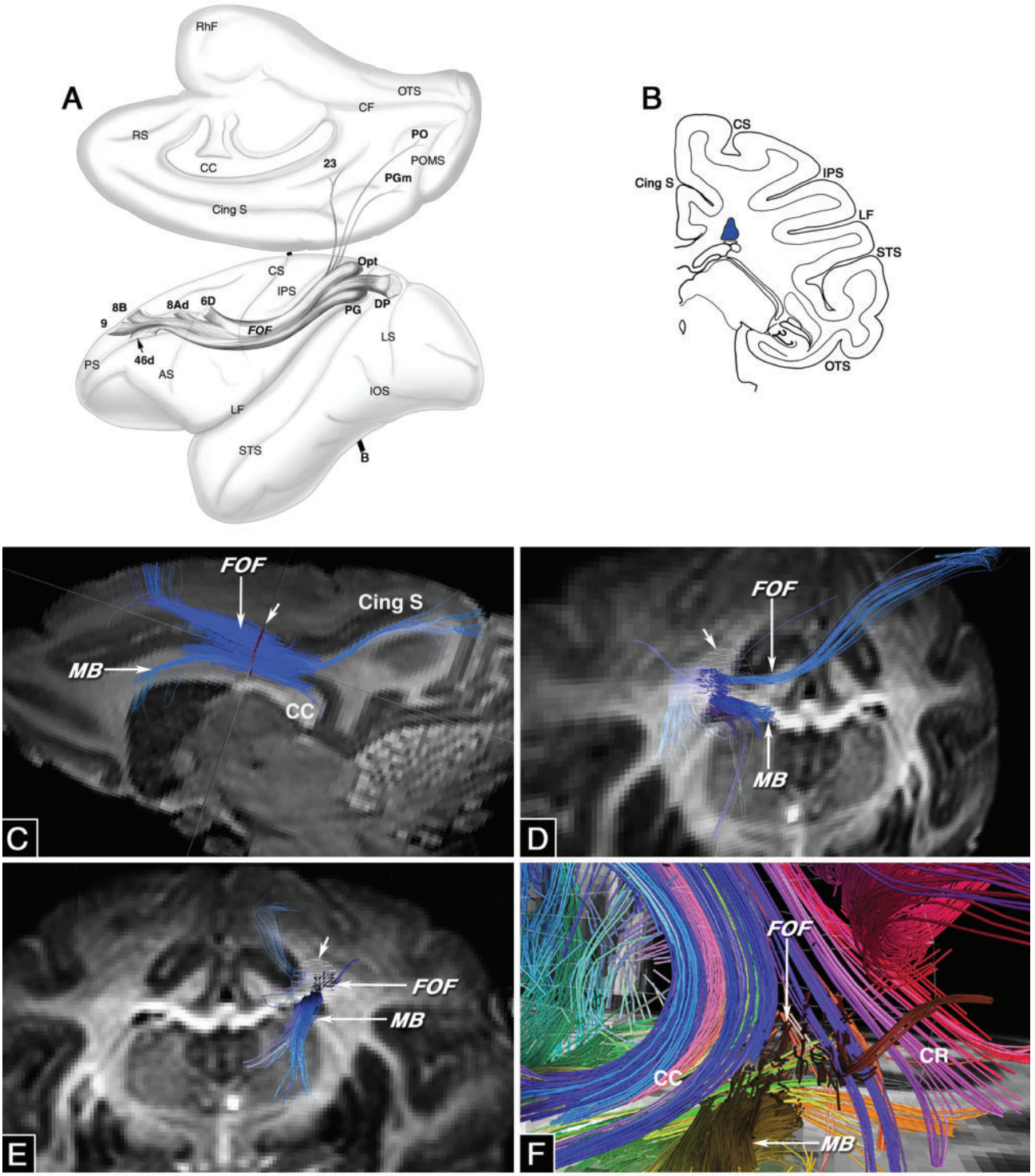

Fig. 8 Diagrams depicting the FOF as determined by the isotope technique (**A, B**) and the FOF and the subcallosal fasciculus of Muratoff (MB) as determined by the DSI technique (**C–F**). (**A**) Surface view of the medial (above) and lateral convexity (below) of the monkey cerebral hemisphere shows the trajectory of the FOF reflected onto the cortical surface, and the cortical areas that it links. (**B**) Coronal section through the cerebral hemisphere of the rhesus monkey taken at the level demarcated in **A** shows the location of the FOF fibre bundle (blue filled area). (**C**) The fibres of the FOF and MB that intersect the disc (short arrow) are shown against a DWI image of the cerebral hemisphere in the sagittal plane. MB fibres descend into the striatum, whereas FOF fibres continue rostrally to the dorsolateral prefrontal cortex. (**D**) Oblique coronal depiction of the FOF and MB fibres that intersect the disc (short arrow) in the rostral caudal dimension, superimposed upon a DWI image of the cerebral hemisphere. This image is viewed from behind the disc. (**E**) End-on view of fibres in the location of the FOF and the MB coursing through the disc (short arrow) in the rostral–caudal direction seen with reference to a DWI coronal section of the cerebral hemisphere, as viewed from a location anterior to the disc. (**F**) High power view in the coronal plane shows the FOF and the MB with reference to the fibres of the corpus callosum and the corona radiata. See list of abbreviations. Fig. 8 (A) reproduced from Schmahmann and Pandya, 2006.

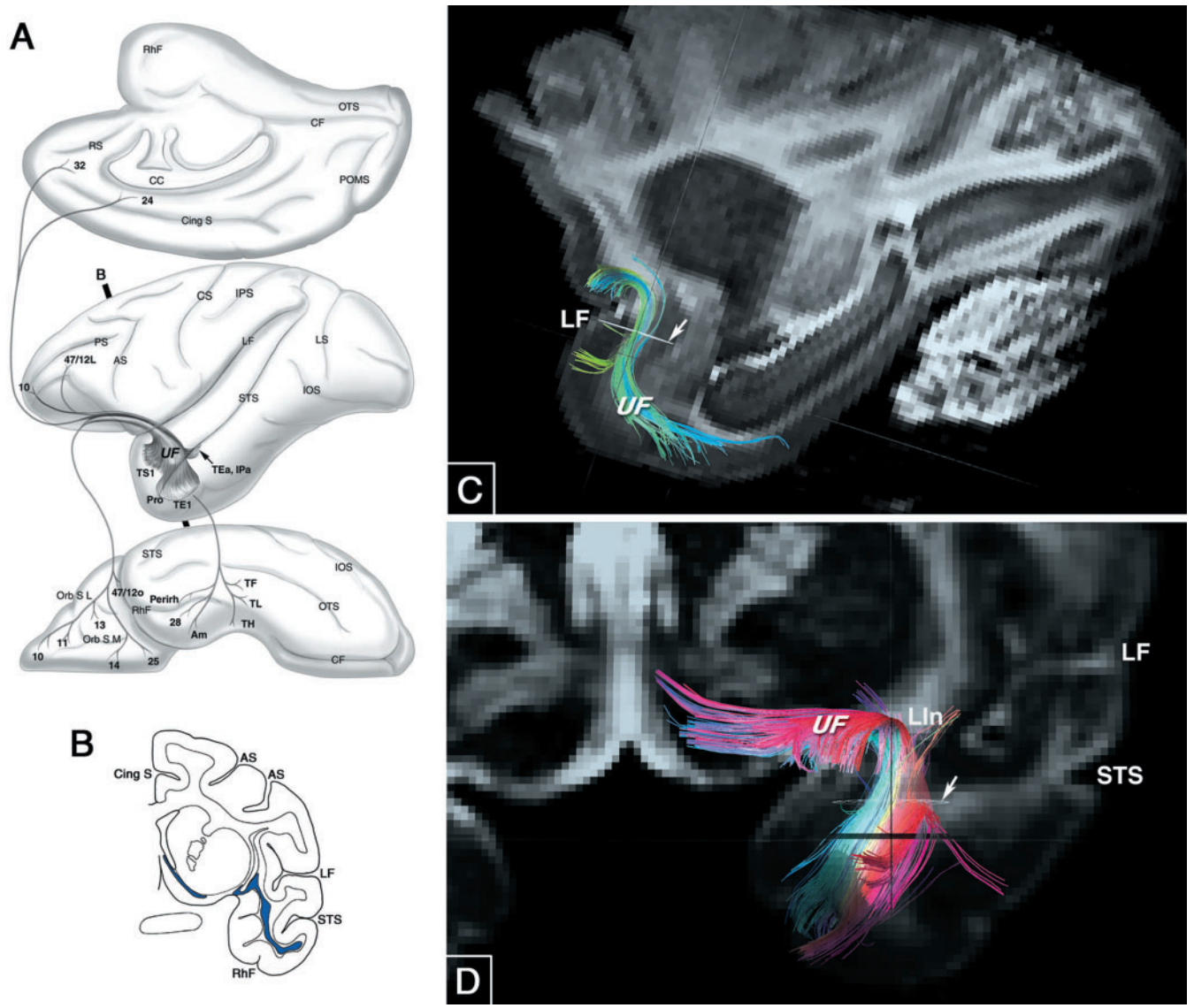

Fig. 9 Diagrams depicting the UF as determined by the isotope (**A, B**) and DSI techniques (**C, D**). (**A**) Views of the medial (top), lateral (middle) and ventral (lower) surfaces of the cerebral hemisphere of the rhesus monkey show the trajectory of the UF reflected onto the cortical surface, and the cortical areas that it links. (**B**) Coronal section through the cerebral hemisphere of the rhesus monkey taken at the level demarcated in A shows the location of the UF fibre bundle (blue filled areas). (**C**) UF fibres intersecting the disc (arrow) are shown in the rostral caudal dimension superimposed upon a DWI sagittal view of the cerebral hemisphere. (**D**) End-on view of fibres in the location of the UF that intersect the disc (arrow) as they course through the L In in the rostral–caudal and mediolateral directions seen with reference to a partial image of a DWI coronal section taken through the frontal and temporal lobes. See list of abbreviations. Fig. 9 (A) reproduced from Schmahmann and Pandya, 2006.

the superior temporal sulcus (STS), and fibres from areas TH and TL in the parahippocampal gyrus. In the frontal lobe, the ventral lateral component leads to areas 9, 9/46d, 8Ad, 24 and 32. The ventral prefrontal contingent leads to areas 45 and 47/12 (Fig. 10A).

DSI. A sphere was placed at the level of the mid-portion of the EmC deep to the temporal lobe where it lies between the insula and the claustrum (Fig. 10E). On the sagittal image (Fig. 10D), the EmC is seen to occupy a position behind the uncinate fibres in the superior temporal gyrus. These fibres course rostrally towards the frontal lobe where they divide into two components. One extends to the ventral lateral part of the frontal lobe, and the other to the orbital cortex. The fibres in the EmC that are located caudal to the position of the sphere are seen to leave or enter the superior temporal region (Fig. 10D and E). In this way the fibre trajectory of the EmC on DSI corresponds to that observed with the isotope technique.

Arcuate fasciculus (AF)

Isotope. The autoradiographic technique shows the trajectory of the AF coursing between the caudal part of the temporal lobe and the frontal lobe (Fig. 11A). It lies in

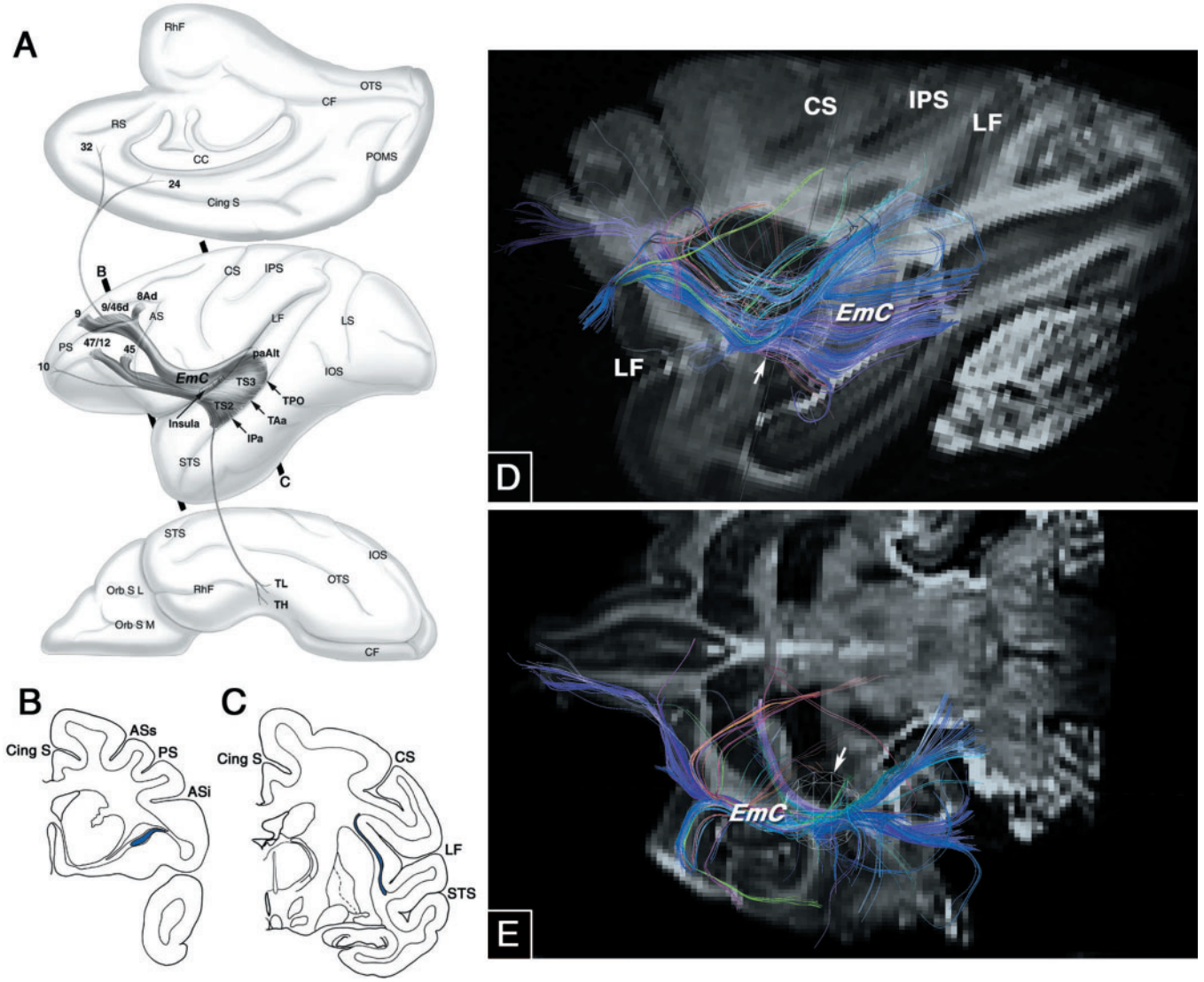

Fig. 10 Diagrams depicting the EmC as determined by the isotope (**A–C**) and DSI techniques (**D, E**). (**A**) Surface views of the medial (top), lateral (middle) and ventral convexities (lower) of the cerebral hemisphere of the rhesus monkey show the trajectory of the EmC reflected onto the cortical surface, and the cortical areas that it links. (**B**) Rostral and (**C**) more caudal coronal sections through the cerebral hemisphere of the rhesus monkey taken at the levels demarcated in **A** to show the location of the EmC fibre bundle (blue filled areas). (**D**) Sagittal view and (**E**) horizontal depiction of EmC fibres shown in the rostral–caudal dimension passing through a sphere (arrows) superimposed upon DWI images of the cerebral hemisphere. See list of abbreviations. Fig. 10 (A) reproduced from Schmahmann and Pandya, 2006.

the white matter deep to the upper shoulder of the sylvian fissure, beneath and adjacent to the SLF II fibres (Fig. 11B). In the frontal lobe, the AF fibres course deep to the white matter of the lateral premotor and lateral prefrontal cortex. In the temporal lobe, the fibres extend into area Tpt of the caudal superior temporal gyrus and area TPO of the STS (Fig. 11A). In the frontal lobe, the fibres of this bundle reach dorsal premotor area 6, dorsal area 8 (8Ad) and dorsal prefrontal area 9/46. Thus this fibre tract interconnects the caudal superior temporal region, that is area Tpt and TPO, and the caudal parts of the dorsal premotor and prefrontal regions.

DSI. The AF can be identified on DSI by placing a sphere in the caudal part of the superior temporal gyrus and the inferior parietal lobule. A group of fibres, in the location of the AF, arches around the caudal end of the sylvian fissure and courses in the caudal part of the superior temporal gyrus (Fig. 11C and D). We were not able to identify with certainty whether the fibres lying obliquely in the caudal part of the superior temporal gyrus were continuous with those that also intersect the sphere and that course in the rostral–caudal plane in the parietal lobe. Thus, the rostral course of the AF fibres into the dorsal part of the premotor and prefrontal area as seen in the isotope

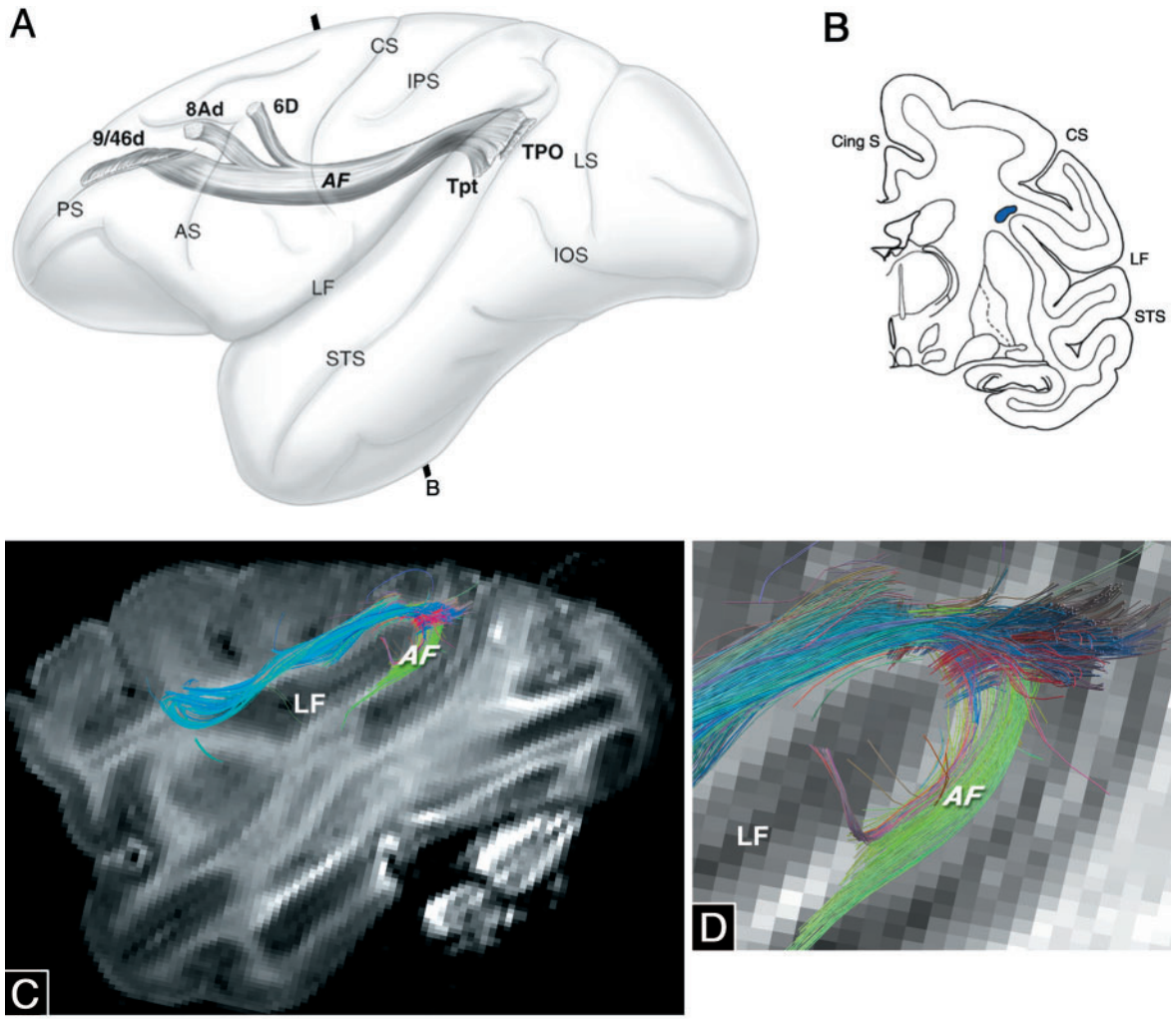

Fig. 11 Diagrams depicting the AF as determined by the isotope (**A, B**) and DSI techniques (**C, D**). (**A**) The surface view of the lateral convexity of the cerebral hemisphere of the rhesus monkey shows the trajectory of the AF reflected onto the cortical surface, and the cortical areas that it links. (**B**) Coronal section through the cerebral hemisphere of the rhesus monkey taken at the level demarcated in A to show the location of the AF fibre bundle (blue filled area). (**C**) Shows DSI fibres that intersect with a sphere placed in the caudal part of the superior temporal gyrus and the inferior parietal lobule. (**D**) A higher magnification view of fibres that arch around the caudal end of the sylvian fissure, in the location of the AF. See list of abbreviations. Fig. 11 (A) reproduced from Schmahmann and Pandya, 2006.

material could not adequately be distinguished on DSI from the SLF II and SLF III fibres that travel into the frontal lobe.

Middle longitudinal fasciculus (MdLF)

Isotope. The autoradiographic material reveals a distinct fibre bundle, the MdLF, coursing within the white matter of the superior temporal gyrus (Fig. 12B and C), extending from the inferior parietal lobule to the temporal pole (Fig. 12A). The MdLF links caudal with rostral sectors within the superior temporal region. It conveys fibres between the superior temporal gyrus including area paAlt; areas TPO, PGa, IPa and TAa in the STS; and areas paAc, proK, paAr and insular Pro within the cortex of the sylvian fissure (Fig. 12A). It also conveys fibres from the caudal cingulate gyrus areas 23 and 30, the dorsal prelunate region area DP, parietal area PG-Opt and the middle sector of the parahippocampal gyrus, towards the multimodal cortex (area TPO and PGa) in the upper bank of the STS. In addition, fibres arise from the lateral and orbital prefrontal cortices and travel caudally within MdLF to terminate in area TPO. The MdLF, therefore, links associative and paralimbic cortices in the inferior parietal lobule, cingulate and prefrontal regions with multimodal parts of the superior temporal region and the parahippocampal gyrus.

DSI. A disc placed in the caudal part of the white matter of the superior temporal gyrus intersects fibres running the length of the superior temporal gyrus and that conform to the location of the MdLF (Fig. 12D). This sizeable bundle extends from the white matter of the inferior parietal lobule to the rostral aspect of the superior

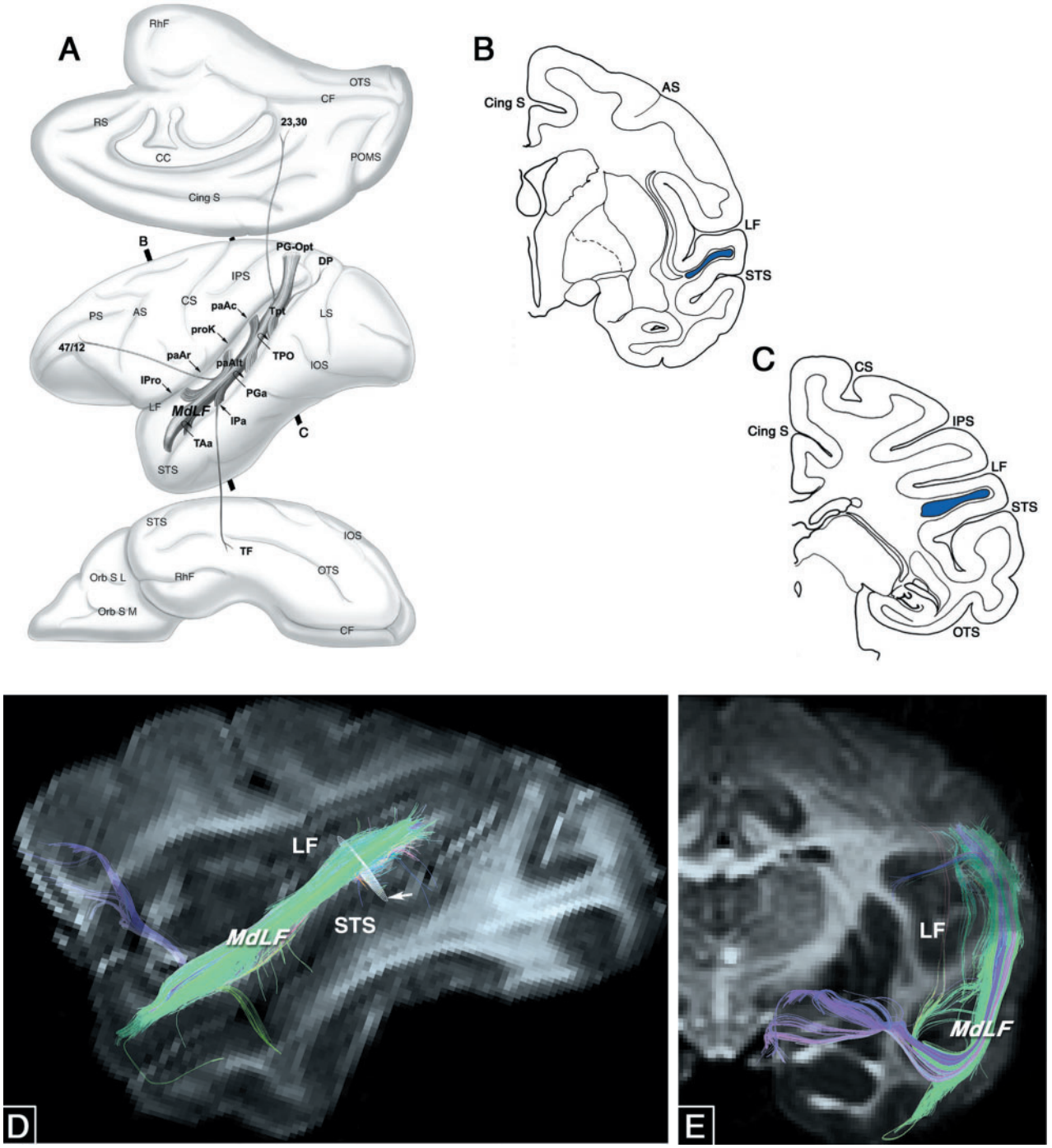

Fig. 12 Diagrams depicting the MdLF as determined by the isotope (**A–C**) and DSI techniques (**D, E**). (**A**) Surface views of the medial (top), lateral (middle) and ventral convexities (lower) of the cerebral hemisphere of the rhesus monkey show the trajectory of the MdLF reflected onto the cortical surface, and the cortical areas that it links. (**B**) Rostral and (**C**) more caudal coronal sections through a hemisphere of the monkey brain taken at the levels demarcated in **A** show the location of the MdLF fibre bundle (blue filled areas) coursing in the white matter of the superior temporal gyrus. (**D**) MdLF fibres intersecting the disc (arrow) placed in the white matter of the superior temporal gyrus are shown in the rostral caudal dimension superimposed upon a DWI sagittal view of the cerebral hemisphere. (**E**) End-on view of fibres in the location of the MdLF coursing in the rostral-caudal direction seen with reference to a DWI coronal section of the cerebral hemisphere. See list of abbreviations. Fig. 12 (A) reproduced from Schmahmann and Pandya, 2006.

temporal gyrus. In the sagittal (Fig. 12D) and coronal (Fig. 12E) images, smaller fascicles emerge from the MdLF directed towards the STS and the sylvian fissure. Fibres that course medially from the rostral aspect of the MdLF may represent fibres of the EmC that, according to the autoradiographic observations, link the prefrontal cortex with the mid-portion of the superior temporal region before continuing into the MdLF.

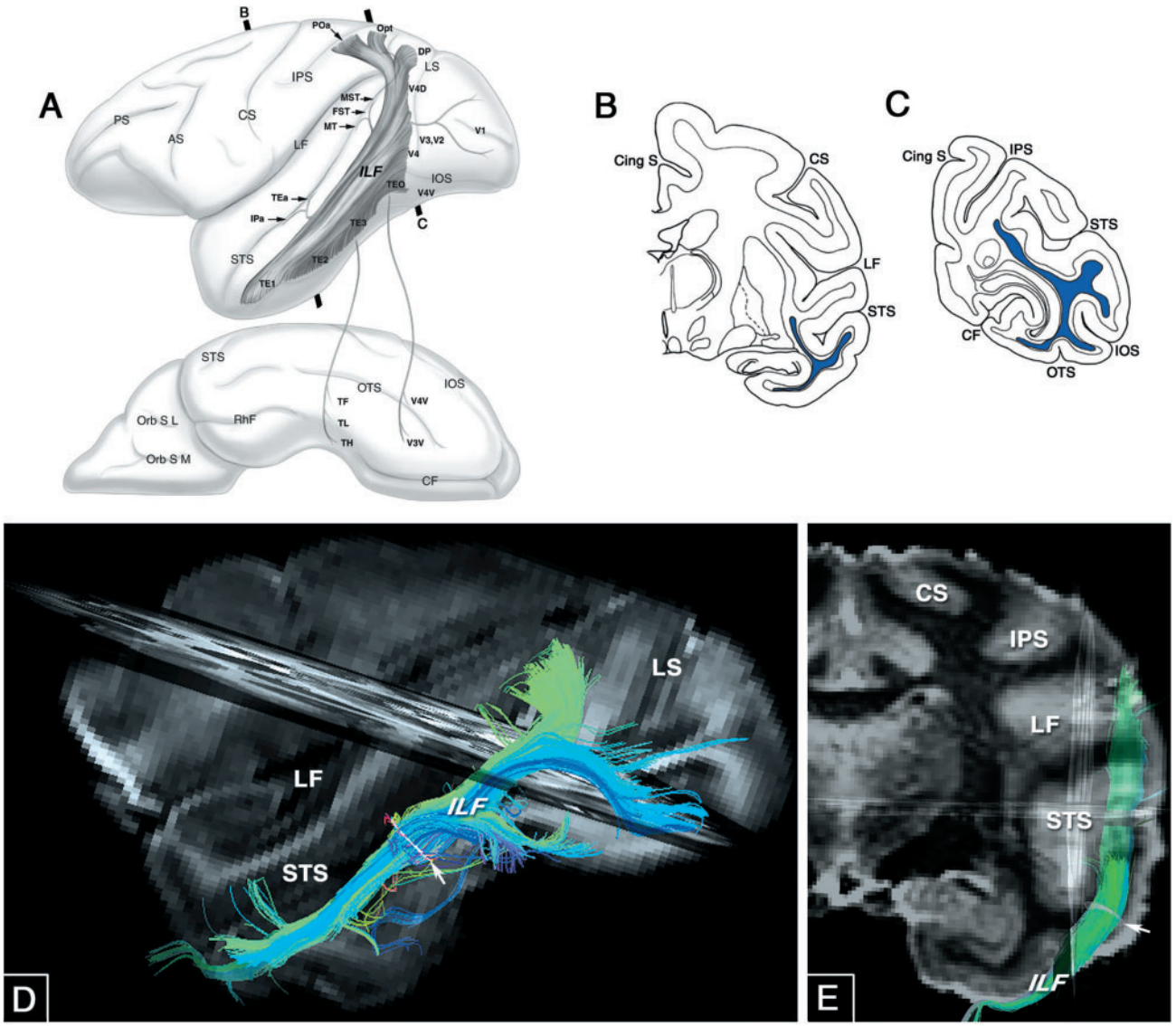

Fig. 13 Diagrams depicting the ILF as determined by the isotope (**A–C**) and DSI techniques (**D, E**). (**A**) Surface views of the lateral (top) and ventral convexity (lower) of the cerebral hemisphere of the rhesus monkey show the trajectory of the ILF reflected onto the cortical surface, and the cortical areas that it links. (**B**) Rostral and (**C**) caudal coronal sections through the cerebral hemisphere of the rhesus monkey taken at the levels demarcated in **A** show the location of the ILF fibre bundle (blue filled areas). (**D**) ILF fibres intersecting the disc (arrow) are shown in the rostral caudal dimension superimposed upon sagittal and oblique horizontal views of the cerebral hemisphere. (**E**) End-on view of ILF fibres coursing in the rostral and caudal directions intersecting the disc (arrow) placed in the white matter of the inferior temporal gyrus, seen with reference to a DWI coronal section of the cerebral hemisphere. See list of abbreviations. Fig. 13 (A) reproduced from Schmahmann and Pandya, 2006.

Occipitotemporal region

Inferior longitudinal fasciculus (ILF)

Isotope. The autoradiographic technique reveals the ILF as a long association fibre tract situated in the white matter of the occipital, parietal and temporal lobes (Fig. 13A–C). It is comprised of a vertical limb caudally, and a horizontal limb ventrally and rostrally. In the parieto-occipital region the ILF fibres run vertically, bounded medially by the sagittal stratum, and laterally by the U-fibres of the parietal, occipital and temporal lobes. At the ventral aspect of the occipital-temporal lobe the ILF fibres course horizontally along the rostrocaudal axis of the temporal lobe, giving off fibres medially to the ventromedial temporal areas and laterally to the inferotemporal region.

The ILF is related to areas POa and Opt in the parietal lobe (Fig. 13A), dorsal parastriate area DP, and areas V4D and V4 in the occipital region, the extrastriate visual areas MST, FST and MT in the STS, and areas TEa and IPa in the rostral part of the STS. The fibres that course through the inferotemporal region relate sequentially to areas TEO, TE3, TE2 and TE1 in the caudal to rostral direction.

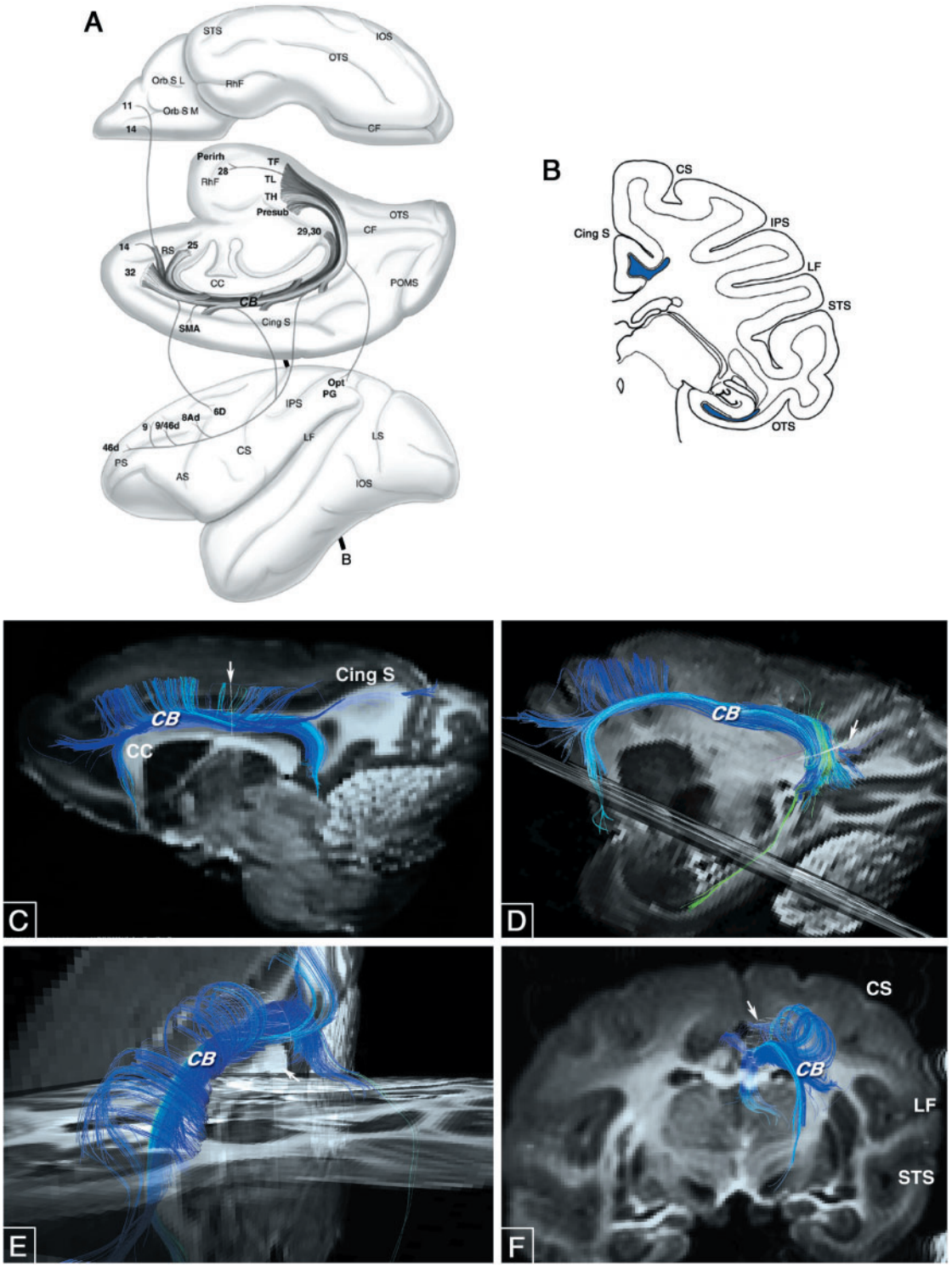

Fig. 14 Diagrams depicting the CB as determined by the isotope (**A, B**) and DSI techniques (**C–F**). (**A**) Surface views of the ventral (top), medial (middle) and lateral (lower) convexities of the cerebral hemisphere of a rhesus monkey show the trajectory of the CB reflected onto the cortical surface, and the cortical areas that it links. (**B**) Coronal section through the cerebral hemisphere of a rhesus monkey taken at the level demarcated in **A** to show the location of the dorsal and ventral components of the CB fibre bundle (blue filled areas). (**C**) CB fibres intersecting the disc (arrow) placed in the white matter of the cingulate gyrus are shown in the rostral–caudal dimension superimposed upon a DWI sagittal view of the cerebral hemisphere. (**D**) CB fibres are shown in the sagittal dimension intersecting the disc (arrow) placed more caudally in the retrosplenial white matter, including fibres in the ventral limb of the CB coursing into the parahippocampal region. (**E**) Oblique anterior view of the CB fibres intersecting the caudally positioned disc (arrow), superimposed upon images in the sagittal and horizontal planes. (**F**) End-on view of fibres in the CB intersecting the disc (arrow) coursing in the rostral–caudal direction in the white matter of the cingulate gyrus, seen with reference to a coronal slice of the cerebral hemisphere. See list of abbreviations. Fig. 14 (A) reproduced from Schmahmann and Pandya, 2006.

A component arising from the inferotemporal region moves medially and relates to the parahippocampal gyrus areas TF, TL and TH. Ventral occipital lobe fibres enter the ILF from areas V4V and V3V. The ILF also extends caudally into the lateral and ventral occipital lobe, and abuts the intrinsic occipital lobe fibre tracts leading to areas V1, V2 and V3.

DSI. Following the placement of the disc in the mid-portion of the white matter of the inferior temporal gyrus, a prominent fibre bundle consistent with the ILF is identified coursing in the rostral–caudal direction (Fig. 13D). It has a vertical component in the parietal lobe, and a horizontal component that lies within the white matter of the occipital and inferior temporal regions (Fig. 13E). The ILF extends from the occipital, inferior parietal and inferotemporal regions all the way up to the temporal pole. Contributing fibres also arise from the occipital, parietal and ventral temporal regions, and from regions that seem to correspond to the STS. Thus, the DSI depiction of the ILF closely matches the observations from the isotope material.

Cingulate gyrus

Cingulum bundle (CB)

Isotope. The CB lies within the white matter of the cingulate gyrus (Fig. 14A and B) and stretches from the frontal lobe around the rostrum and genu of the corpus callosum (CC), extending caudally above the body of the CC before curving ventrally around the splenium of the CC to lie in the white matter of the parahippocampal gyrus (Fig. 14A and B). CB fibres rostrol through caudal sectors of the cirgulate gyrus, and in the frontal lobe they arise from or terminate in areas 11 and 14 on the orbital surface, and areas 25 and 32 medially (Fig. 14A). Fibres directed rostrally and laterally in the frontal lobe lead to the SMA and areas 8, 9 and 46 in the dorsolateral prefrontal cortex. CB fibres leading to the parietal lobe arise from or terminate in the caudal inferior parietal lobule, area PG/Opt, and medially in the retrosplenial cortex, areas 29 and 30. Fibres in the CB that curve around the splenium of the CC towards the parahippocampal region lead to areas TF, TL and TH and the presubiculum of the parahippocampal gyrus, as well as the entorhinal and perirhinal region. Fibres arch up from the CB and terminate locally in the cingulate gyrus.

DSI. The CB is readily identified with the DSI approach. When the disc is placed within the white matter of the middle or caudal parts of the cingulate gyrus, the dorsal limb of the CB is shown within the white matter of the cingulate gyrus (Fig. 14C–F). When the disc is placed around the retrosplenial white matter, the ventral limb of the CB within the white matter of the parahippocampal gyrus is also evident (Fig. 14D). The CB fibres extend rostrally into the lateral and medial frontal lobes, and caudally into the parietal lobe. Fibres that arch ventrally around the splenium continue through the entire length of the white matter of the parahippocampal gyrus. The fibres that loop above the CB lead to and contribute to the cingulate gyrus (Fig. 14C–F), as in the isotope study.

Discussion

We have identified the trajectories of the major cortical association fibre bundles of the monkey cerebral hemisphere with magnetic resonance DSI, and compared the results with those derived from histological tract tracing.

This study was prompted by two developments. First, the recently available exposition of the white matter architecture of the cerebral hemisphere of the rhesus monkey (Schmahmann and Pandya, 2006) provides a data set against which the results of the DSI investigation may be compared in order to assess the validity of this new imaging approach.

Second, the ability of DSI to resolve crossing fibres within a given voxel represents a substantial advance in the ability of MRI to determine the complex organization of cerebral white matter. The results of the present study validate the DSI technique because they closely reflect the definitive findings from the autoradiographic tract tracing study. Whereas DSI has lower resolution than the isotope technique, it has advantages that are not yet possible to attain using the histological material. With DSI it is possible to examine fibre tracts in multiple planes of section, and in 3D space it can define their course and relationships to other structures. The trajectory of the fibre tract in DSI is an actual depiction of the data, not a 3D representation of primary connectional data superimposed upon a 2D image of the lateral hemisphere. DSI also has the potential advantage of being able to identify a fibre bundle *in vivo* as well as *in vitro*, a desirable goal with clinicopathological relevance.

The power of the DSI approach to disentangle fibres with intersecting trajectories is perhaps most readily demonstrated by its ability to identify the fibres of the FOF and the subcallosal fasciculus of Muratoff that travel in the horizontal dimension, and to distinguish them from the vertically oriented fibres of the corona radiata, and the mediolaterally directed fibres of the CC (as seen in Fig. 8C–F). The arrangement shown with DSI reflects the anatomic reality observed in histological tract tracing studies. The identification of these tracts is of no trivial importance. There has been considerable debate regarding the existence, course and composition of the MB and the FOF. The isotope study, supported now by the DSI analysis, reveals that the MB is purely a corticostriate fasciculus, whereas the FOF is a long association pathway linking the frontal lobe with the parieto-occipital region and it also has some input to the MB.

Putative functional attributes of the identified fibre pathways

By accurately depicting the cortical origins, trajectories and destinations of the fibre pathways it is possible to develop

new insights into the putative functional properties subserved by these tracts. We consider these here in order to emphasize the relevance of the anatomic approach for understanding the contributions of the participating components of the distributed neural circuits.

Superior longitudinal fasciculus (SLF)

The SLF I is shown by autoradiography and DSI to link the superior parietal lobule important for appreciating limb and trunk location in body-centred coordinate space, with the premotor areas engaged in the higher aspects of motor behaviour and the SMA important for intention and the initiation of motor activity. The SLF I may thus be regarded as relevant to the higher order control of body-centred action, and for the initiation of motor activity (Petrides and Pandya, 2006; Schmahmann and Pandya, 2006).

The SLF II courses between the caudal part of the inferior parietal lobule and IPS concerned with visual–spatial information, and the posterior prefrontal cortices important for perception and awareness. This pathway thus appears to be relevant in spatial attention, and the feedback from frontal lobe to parietal lobe in particular may be involved in focusing spatial attention (Petrides and Pandya, 2006; Schmahmann and Pandya, 2006). Lesions of the parietal lobe in patients (Denny-Brown *et al.*, 1952; Critchley, 1953) and monkeys (Heilman *et al.*, 1970) result in disorders of spatial awareness including hemi-inattention and neglect. The distributed neural circuitry (network) approach to the localization of complex functions applied to the phenomenon of spatial attention (Mesulam, 1981) holds that in the right hemisphere of dextrals there is functional specialization for the distribution of directed attention within extrapersonal space, a function in which the parietal lobe plays a pivotal role. Behavioural studies in monkeys demonstrate that parietal leucotomy, i.e. disruption of the parietal lobe white matter between the fundus of the IPS and the lateral ventricle, results in severe hemispatial neglect (Gaffan and Hornak, 1997). The lesion in that study was well placed to disrupt the SFL II in particular, consistent with the hypothesis that SLF II is important in spatial awareness. Other fascicles likely to be spatially relevant that may have been disrupted include the FOF (see below), and the superior aspect of the sagittal stratum that contains dorsal parastriate and posterior parietal lobe connections with thalamus and pons (Schmahmann and Pandya, 2006).

Isotope and DSI both reveal that the SLF III links the following areas: the rostral inferior parietal lobule, an intramodal association area concerned with high order somatosensory information that is equivalent in human to the supramarginal gyrus; the ventral premotor area (area 6 and area 44—equivalent in human to the pars opercularis) that contains mirror neurons important for action imitation (Rizzolatti *et al.*, 1999; Ferrari *et al.*, 2003), and lesions in this area result in cortical dysarthria, aphemia and oral and buccal apraxias (Schiff *et al.*, 1983; Grosswasser *et al.*, 1988; Maeshima *et al.*, 1997; Woolley, 2003); and ventral prefrontal area 46 that is engaged in working memory. By providing connections between these cortical areas, the SLF III is likely to be involved in the gestural component of language, and in orofacial working memory (Preuss and Goldman-Rakic, 1989).

Fronto-occipital fasciculus

The controversy surrounding the existence of the FOF in monkey appears to have been resolved by the detection of this fibre tract with the isotope technique. DSI has now also clearly identified and isolated the FOF from the surrounding fibre bundles. In monkey the FOF is situated above the subcallosal fasciculus of Muratoff (a corticostriate fibre bundle), and between the corona radiata laterally and the fibres of the CC medially. The FOF long association bundle courses between the dorsal and medial parastriate and caudal posterior parietal cortices that are important for peripheral vision and visual motion, and the dorsolateral prefrontal cortex including area 8 that is necessary for attention. These attributes confer upon the FOF a role in visual spatial processing (Galletti *et al.*, 2001; Rizzolatti and Matelli, 2003; Schmahmann and Pandya, 2006).

Both the isotope and DSI techniques thus demonstrate that the FOF long association bundle and the MB corticostriatal fasciculus can be differentiated by virtue of their location and their connections. It should be noted that the isotope study also demonstrates some fibres in the FOF that descend into the MB before terminating in the striatum, and thus a small contingent of corticostriatal fibres course in the FOF. In contrast, there are no cortico-cortical association fibres lying within the MB.

Early investigators (e.g. Meynert, 1885; Dejerine, 1895) were unable to distinguish the MB and FOF from each with the available techniques, and they could not satisfactorily ascertain their course and constituent fibres. These discussions were further compounded by considering the 'FOF' of Forel and Onufrowicz (1887) to be a normal anatomical bundle, whereas this was nothing more than misplaced callosal fibres in cases of callosal agenesis. The confusion of the FOF and the MB, at least in monkey, has now been resolved by the evidence derived from autoradiography and our DSI study. It remains to be shown how well these findings in the monkey relate to the FOF and MB in the human.

Our isotope and DSI studies in monkey do not provide evidence in support of an 'inferior' FOF, and therefore we have not perpetuated the use of the term 'superior FOF'. Our findings, together with the lack of evidence in prior connectional studies in monkey of a pathway leading from ventral sectors of the occipital lobe to the orbital frontal cortex, lead us to a position that is not yet reconcilable with that of gross dissection (Trolard, 1906; Curran, 1909; Davis, 1921; Ludwig and Klingler, 1956; Heimer, 1995) and DTI

studies (Catani *et al.*, 2002; O'Donnell *et al.*, 2006; Taoka *et al.*, 2006) in the human indicating the presence of such an inferior FOF. We have postulated previously (Schmahmann and Pandya, 2006) that the apparent existence of an 'inferior FOF' may result from conflation of the ILF caudally with the EmC and/or UF rostrally, spuriously producing the appearance of a continuous association fibre bundle. Resolution of this issue has important theoretical implications, because it would imply either that one of these opposing conclusions is erroneous, or a novel pathway has arisen in humans that is not present in monkey.

The uncinate fasciculus

Both the autoradiographic technique and DSI reveal the UF coursing between the rostral temporal region and the orbital and medial prefrontal cortices. The UF is a ventral limbic pathway that links the rostral superior temporal gyrus important for sound recognition (Clarke *et al.*, 2002), the rostral inferior temporal gyrus that supports object recognition (Spiegler and Mishkin, 1981; Baylis and Rolls, 1987; Tsao *et al.*, 2003; Kellenbach *et al.*, 2005), the medial temporal area (entorhinal, perirhinal, parahippocampal gyrus) relevant in recognition memory (Mishkin, 1982; Squire and Zola-Morgan, 1991), and the orbital, medial and prefrontal cortices involved in emotion, inhibition and self-regulation (Butter *et al.*, 1970; Bechara *et al.*, 1994; Levine *et al.*, 2002). The UF appears to be critical for processing novel information, understanding emotional aspects of the nature of sounds and for self-regulation including the regulation of emotional responses to auditory stimuli (Frey *et al.*, 2000). These connections provide support for the notion that the UF enables the interaction between emotion and cognition (MacLean, 1952; Barbas, 2000).

Behavioural studies in monkeys also suggest that the UF may be critical in visual learning. Bilateral lesions of the anterior temporal stem (through which the UF runs), the amygdala and fornix produce severe anterograde amnesia (Gaffan *et al.*, 2001). Lesions of the frontal and temporal lobes on opposite sides, effectively producing frontal–temporal disconnection subserved by the UF, abolish learning and suggest that fronto–temporal disconnection impairs the process of representing temporally extended events (Browning *et al.*, 2006). Additionally, lesions in monkeys of the cholinergic basal forebrain and the inferior temporal cortex (a connection subserved also by the UF) produce severe impairments in learning visual scenes and object-reward associations (Easton *et al.*, 2002).

Clinical reports suggest that damage to the UF produces disruption of temporal–frontal connections resulting in disordered self-regulation. A patient with damage to the right ventral frontal cortex and underlying white matter including the UF developed dense amnesia for experiences predating the lesion, and he experienced impairment of autonoetic awareness, i.e. awareness of oneself as a continuous entity across time that supports the formulation of future goals and the implementation of a behavioural guidance system to achieve them (Levine *et al.*, 1998). The role of the UF has been addressed in schizophrenia (Highley *et al.*, 2002; Kubicki *et al.*, 2002), and functional connectivity between the frontal and temporoparietal regions has been reported to be disturbed in schizophrenia patients and in subjects at genetic risk for the disorder (Winterer *et al.*, 2003). The UF may be relevant also in the interictal personality disorder of temporal lobe epilepsy. In patients with seizures, temporal lobectomy lowers seizure frequency by excision of the epileptic focus (e.g. Glaser, 1980; Rasmussen, 1980), and it improves psychosocial outcome and aggressive and antisocial behaviours in some children and adults (Hill *et al.*, 1957; Helmstaedter *et al.*, 2003; Nakaji *et al.*, 2003; Ettinger, 2004). Perhaps this improvement following temporal lobectomy occurs because the UF is no longer able to convey pathological information from the temporal lobe to the decision-making regions of the medial and orbitofrontal cortices. This would be analogous to the beneficial effects of cingulotomy (e.g. Ballantine *et al.*, 1987; Cosgrove and Rauch, 2003). This hypothesis remains to be tested. It may also be useful to study the UF in surgical and autopsy specimens by taking advantage of its chemical specificity demonstrated using acetylcholine staining (Selden *et al.*, 1998).

Extreme capsule

The results of the study utilizing the isotope technique in monkey, confirmed in large part by DSI, reveals that the EmC is an association fibre pathway, as noted also previously in the human (Crosby *et al.*, 1982). The EmC is distinguished from the external capsule situated between the claustrum and putamen, that according to experimental observations (Schmahmann and Pandya, 2006) is strictly a corticostriatal fibre tract. The EmC links the cortex of the STS (area TPO), superior temporal gyrus (area paAlt), supratemporal plane and insula with the frontal lobe area 45, area 47 on the orbital cortex and the dorsolateral prefrontal cortex. Area paAlt and the mid-part of area TPO are homologous with Wernicke's area in the human, and area 45 is homologous to Broca's area (pars triangularis) in the human. The connection between Broca's and Wernicke's areas is important in the linguistic (non-articulatory) aspects of language communication, and this link has long been considered to be conveyed by the AF (Wernicke, 1874; Lichtheim, 1885; Dejerine, 1895; Geschwind, 1965). Damage to the AF is thought to be the anatomic underpinning of conduction aphasia. Our results in the monkey, however, suggest that it is the EmC, and not the AF, that perhaps enables the interaction between the cortices that are homologous to these language areas. These findings may be compounded by species differences between human and monkey, as functional differences between these two species are likely to be

associated with important anatomical differences as well. This notwithstanding, the present observations raise an interesting debate (see below). Our results suggesting that the EmC rather than the AF may be important in conduction aphasia is amenable to being solved in the human by the use of DSI.

Arcuate fasciculus

The DSI technique was able to visualize part of the trajectory of the AF as the fibres arch around the caudal end of the sylvian fissure into the superior temporal gyrus, but was unable to confirm that these fibres are continuous with those coursing into the frontal lobe. The isotope study, however, indicates that the AF links the caudal superior temporal gyrus involved in sound localization (e.g. Leinonen *et al.*, 1980; Rauschecker *et al.*, 1995) with the caudal dorsal prefrontal cortex involved in spatial attention (Suzuki and Azuma, 1977; Goldberg and Segraves, 1987) and working memory (Preuss and Goldman-Rakic, 1989). According to the present results, the AF does not link the mid-superior temporal region with the cortex homologous to Broca's area, namely area 45. The connectional data thus suggest that the AF is important in spatial processing in the auditory domain, perhaps signalling the location and directionality of sounds including those relevant for language, but is not involved in the symbolic representations of language itself. This is a somewhat heretical notion, given the long history of the relationship of the AF to conduction aphasia, discussed above. Nevertheless, the anatomy in the monkey makes the case that it is the EmC and MdLF (see below) and not the AF that are involved in language. Furthermore, lesion-deficit studies in humans are unlikely to involve any of these three fibre bundles in isolation. Therefore, using the present observations in the monkey as a starting point, the application of DSI to the human may help further define the actual role of the AF.

Middle longitudinal fasciculus

Another novel observation with the DSI method that confirms the findings with isotope tract tracing is the extent of a fibre bundle coursing rostrocaudally in the white matter of the superior temporal gyrus—the MdLF (Seltzer and Pandya, 1984; Schmahmann and Pandya, 2006). The isotope study shows that the MdLF links associative and paralimbic cortices in the parietal, cingulate, parahippocampal and prefrontal regions with multimodal cortices of the superior temporal region. As a multimodal and supramodal association bundle, these rich interconnections are likely to facilitate such high level functions as spatial organization, memory and motivational valence. In addition, our tract tracing study and DSI analysis reveal fibres in the MdLF travelling between the inferior parietal lobule and the superior temporal region. These findings have relevance for recent observations derived from DTI suggesting that a caudal, vertical limb of the AF conveys the connection between the angular gyrus and the superior temporal gyrus (Catani *et al.*, 2005). The fasciculus identified by these authors as a caudal component of the AF could conceivably represent the MdLF of our observations. It will be of interest to study the MdLF in the human because by linking the angular gyrus with the language areas of the temporal cortex, it may play a role in language comprehension, and complement the EmC in facilitating the interaction between the language cortices.

Language and the AF, EmC and MdLF. The AF is traditionally regarded as playing an important role in language genesis in human, connecting Broca's area in the frontal lobe with Wernicke's area in the temporal lobe. Anatomical descriptions of the AF have been central in the understanding of neural systems that subserve language, and this conclusion has received support from lesion-deficit studies of conduction aphasia (Wernicke, 1874; Dejerine, 1895; Barker, 1899; Liepmann—see Geschwind, 1965; Brown, 1988) and more recently from DTI analyses of the neural correlates of language (e.g. Catani *et al.*, 2005; Anwander *et al.*, 2006). Considerable evidence in the monkey demonstrates connections between the areas of the frontal and temporal lobes that are homologous to Broca's area—ventral prefrontal cortex, area 45 (Petrides and Pandya, 2002)—and Wernicke's area—mid-superior temporal cortex, area paAlt (Schmahmann and Pandya, 2006; Fullerton and Pandya, in preparation). Based on the monkey data arising from the isotope and DSI analyses, however, it appears that the fibres that link the Broca and Wernicke equivalent regions do not course within the AF. Rather, isotope studies indicate that fibres in the AF connect area Tpt in the caudal superior temporal gyrus with the dorsal caudal prefrontal area (area 8; Petrides and Pandya 1988; Schmahmann and Pandya, 2006). In some contemporary discussions, reference is made to ventral prefrontal area 45 receiving input from the superior temporal gyrus including area Tpt (e.g. Aboitiz *et al.*, 2006). However, in experimental material in which the isotope injection is confined to area Tpt and does not involve area paAlt, projections to the frontal lobe are situated in dorsal prefrontal areas and avoid area 45. Physiological studies in non-human primates (Leinonen *et al.*, 1980; Benson *et al.*, 1981; Rauschecker and Tian, 2000), functional imaging studies in humans (Martinkauppi *et al.*, 2000; Rauschecker and Tian, 2000; Wise *et al.*, 2001) and clinical observations (Clarke *et al.*, 2002; Clarke and Thiran, 2004) suggest that the caudal STG is involved in sound localization, and thus the AF that conveys the connections between the caudal STG and the frontal lobe may contribute to sound localization rather than language comprehension.

These observations led us to search for alternative pathway(s) linking the homologous areas of Broca and Wernicke that may be relevant to considerations

of language. In our isotope studies we observed a distinct fibre pathway (the MdLF) confirming the observations of Seltzer and Pandya (1984), leading from the inferior parietal lobule (equivalent to area 39, the angular gyrus) to the auditory association areas of the superior temporal gyrus and the multimodal parts of the STS (Wernicke area precursor). We also observed bidirectional pathways leading from the lower prefrontal region (Broca's area precursor) to the middle part of the superior temporal gyrus and sulcus by way of the EmC. These findings are now replicated to the extent currently possible by DSI. By virtue of their connections with auditory association cortices in the mid-part of the superior temporal gyrus and sulcus, the EmC and MdLF pathways thus appear to be relevant for sound comprehension. We interpret our observations to suggest that these systems that are present in monkey may evolve in humans to provide the substrate for language comprehension.

We realize that these are controversial assertions. Our findings with isotope and DSI are derived from the monkey, whereas those from clinical and pathological study and DTI analyses are based on work in humans. The monkey is certainly not endowed with language, nevertheless, monkeys do communicate, and we subscribe to the notion that language evolved in concert with the evolution of the rudimentary structural elements required for communication. These structural elements include the cortical areas homologous to language, and the pathways that link them, namely, we propose, the EmC and the MdLF. This offers an approach that differs from the existing classical view, and it provides hypotheses that may be tested in humans with increasingly sophisticated imaging techniques, including DSI.

Inferior longitudinal fasciculus

The isotope study demonstrates a long association fibre bundle linking the occipital and temporal lobes, conforming to the ILF. The DSI study further supports these anatomical observations in monkey. Many investigators have confused the ILF with the lateral segment of the sagittal stratum. Experimental investigations reveal that the sagittal stratum is purely a projection system. In contrast, the ILF, which is situated lateral to and is entirely distinct from the sagittal stratum, is in fact predominantly an occipitotemporal association fibre system. Findings from human DTI work (e.g. Catani *et al.*, 2002) also makes it clear that the ILF exists and that it is a long association fibre tract, contrary to earlier conclusions (Tusa and Ungerleider, 1985). Unlike the FOF that plays a role in the dorsal visual stream, the ILF links the ventral and lateral occipital regions concerned with central vision with the ventral temporal cortices important for object recognition, and the posterior parahippocampal gyrus engaged in memory (Ungerleider and Mishkin, 1982; Squire and Zola-Morgan, 1991). The functional properties of these cortical areas confer on the ILF a role in the ventral visual stream, that is, in object recognition, discrimination and memory. Face recognition is likely dependent upon the ILF, and the clinical phenomenon of prosopagnosia may result from its destruction (see e.g. Catani *et al.*, 2003).

The cingulum bundle

In contrast to the UF which is the ventral limbic fibre bundle, the CB is the dorsal limbic pathway. It links the caudal cingulate gyrus with the hippocampus and parahippocampal gyrus critical for memory, prefrontal areas 9 and 46 important for manipulating information and monitoring behaviour and for working memory (Petrides, 1995), and the rostral cingulate gyrus involved in motivation and drive (Stuss and Benson, 1986; Devinsky *et al.*, 1995). The isotope and DSI methods also demonstrate that the CB receives or provides arching fibres to the cingulate gyrus along its course. The CB is thus likely to be crucial for a wide range of motivational and emotional aspects of behaviour, and involved also in spatial working memory. The effect on the highest levels of psychosocial behaviour following disruption of the long association and subcortical connections subserved by the CB has long been appreciated, as exemplified by the earlier use of prefrontal leucotomy (Fulton—see Moniz, 1937; Freeman and Watts, 1942; Pressman, 1988), and the contemporary use of cingulotomy for obsessive compulsive disorder (e.g. Ballantine *et al.*, 1987; Spangler *et al.*, 1996; Cosgrove and Rauch, 2003).

Limitations of the DSI method

DSI is an essentially model-free imaging approach to the mapping of complex neural fibre architecture at the scale of single MRI voxels. The limitations of DSI arise in ways similar or identical to those of other digital imaging methods, as limitations of resolution and signal-to-noise ratios. Resolution in DSI includes both spatial and angular resolution. DSI uses angular resolution to separate fibre populations within a voxel and to measure their 3D orientations. The present experiments of 515 samples have a nominal angular resolution of 15°. Accordingly, they will not resolve separate fibre populations that cross at angles shallower than 15° ['kissing fibres' (Basser *et al.*, 2000)] and they will assign local orientations with an accuracy of ±7°, leading to potential errors of similar size within reconstructed trajectories. DSI spatial resolution is required to resolve curvatures within individual fibre bundles. In the present case, the curvature limit of 0.5 radian per 500 μm voxel means that fibre bundles with radius of curvature <0.6–1.0 mm are not accurately resolved. This limitation may in part be responsible for disconnection of fibre tract solutions at the cortical–subcortical interface, where fibre curvatures may be quite high with radius of curvature <500 μm. The signal-to-noise ratio of these experiments sets a limit to the smallest concentrations of fibres that can be detected. Owing to this limit, DSI will

tend to under-represent components of fibre bundles that fan out, becoming more dilute locally. Given the diffusion anisotropy contrast we find in typical association pathways, present experiments may detect fibre subpopulations with local concentrations $\geqslant$20% per voxel and fail to detect lower concentrations. The DSI method accurately reflects both the stem portions and the tributaries of the pathways, but does not robustly demonstrate the terminations in the cortex, which are seen in some instances, but not in all cases. This may result from a limitation of spatial resolution as the fibres turn abruptly at the subcortical margin, coupled with reduced diffusion contrast as the fibres enter the grey matter and lose their myelin. Improved contrast and resolution in the acquisition of the MRI data may be required in order to demonstrate these terminations.

The comparison of connectivity from isotope studies and from DSI may be even more compelling if one is able to combine these two methodologies in the same brains rather than separately as in our study. The present analysis addresses the overall organization of the pathways rather than their cortical termination sites, and thus the methods employed here are sufficiently accurate to address the primary goal of this investigation.

The protracted imaging time (25 h) and the restrictions on coil size currently limit DSI tract tracing with high signal-to-noise ratio to the study of post-mortem brains of animals such as monkey, or portions of post-mortem human brain. As the technology advances, we are optimistic that it will be possible to perform DSI with excellent spatial resolution in the whole human brain both post-mortem and *in vivo*.

Conclusions

The information gained from isotope studies of the monkey brain with regard to the organization of the association tracts and the cortical areas that they link provided new insights into the functional properties of these pathways, and removed many previously intractable obstacles to the comprehensive understanding of these fibre bundles. The present study shows a remarkable concordance of results between two fundamentally different techniques, isotope tract tracing and DSI, in the evaluation of the organization of the long association pathways of the cerebral white matter in monkey. These demonstrations of the white matter tracts in the monkey amount to a validation of the DSI methodology with reference to the histological technique.

Although many of these fibre tracts have been outlined using DTI, that method has the limitation of being unable to resolve details of crossing fibres. This problem has been resolved to a considerable extent using DSI, that shows crossing fibres in a manner that could previously be seen only with the aid of a microscope after the injection of axonal tracers. A major advantage of the DSI technique, therefore, is that it takes us a step closer to being able to discern the origins, course and destinations of fibre connections in a non-invasive, timely and reliable manner.

This study in monkey has direct relevance for future investigations of the human brain. The histological method facilitates a degree of precision that is still not yet attainable by the imaging techniques. Whereas the veracity of the histological tract tracing technique is incontrovertible, the problem inherent in the monkey data is how well it applies to the understanding of the human brain, particularly when considering such human functions as language and high order executive behaviour. Conversely, the almost instantaneous derivation of visually dramatic results in the human brain using non-invasive imaging is constrained by the underlying uncertainty as to how true and reliable these observations really are. The limitations of tractography derived from the tensor method are well documented (Basser *et al.*, 2000; Tench *et al.*, 2002; Ciccarelli *et al.*, 2003), and like the gross dissection studies of old, they raise the concern that the fibre bundles displayed by these techniques may be artefacts of the methodology.

This sets up an inherent conundrum, that is, the existence of definitive data derived from monkey on the one hand, as opposed to data of uncertain authority obtained in the human on the other. Here we have attempted to resolve this difficulty in the same species, by cross validating the results of our histological investigations with the non-invasive DSI tract tracing technique.

This validation of the DSI method facilitates the application of this technique to the human brain in the normal and diseased state. In its present iteration, both methodologies, tract tracing and DSI, were conducted in post-mortem brains. The signal-to-noise ratio facilitated by the imaging of the post-mortem brain for multiple hours reflects the current state of the DSI technology. As improvements occur in the DSI method facilitated by future technological advancements, it is likely that the increasingly reliable demonstration of white matter pathways in the human brain, together with a greater understanding of the likely functional attributes of these tracts, will help shed light on the neuronal ensembles that form interconnected circuits supporting neurological function.

Acknowledgements

This work has been supported in part by the Birmingham Foundation (J.D.S.), NIH MH64044 (V.J.W.), NIH NS41285 (A.D.C.), AHA EIA0640064N (A.D.C.), the Athinoula A. Martinos Center for Biomedical Imaging (P41RR14075, S10RR016811) and the MIND Institute. The invaluable assistance of Jason MacMore, B.A. is appreciated. Funding to pay the Open Access publication charges for this article was provided by the Birmingham Foundation.

References

Aboitiz F, Garcia R, Brunetti E, Bosman C. The origin of Broca's area and its connections from an ancestral working-memory network. In: Grodzinsky J, Amunts K, editors. Broca's region. New York: Oxford University Press; 2006.

Anwander A, Tittgemeyer M, von Cramon DY, Friederici AD, Knosche TR. Connectivity-based parcellation of Broca's area. Cereb Cortex 2006 May 17. Epub ahead of print.

Au R, Massaro JM, Wolf PA, Young ME, Beiser A, Seshadri S, et al. Association of white matter hyperintensity volume with decreased cognitive functioning: the Framingham Heart Study. Arch Neurol 2006; 63: 246–50.

Ballantine HT, Bouckoms AJ, Thomas EK, Gitiunas IE. Treatment of psychiatric illness by stereotactic cingulotomy. Biol Psychiatry 1987; 22: 807–19.

Barbas H. Connections underlying the synthesis of cognition, memory, and emotion in primate prefrontal cortices. Brain Res Bull 2000; 52: 319–30.

Barker LF. The nervous system and its constituent neurones. New York: D. Appleton and Co.; 1899.

Basser PJ, Mattiello J, LeBihan D. MR diffusion tensor spectroscopy and imaging. Biophys J 1994; 66: 259–67.

Basser PJ, Pajevic S, Pierpaoli C, Duda J, Aldroubi A. In vivo fiber tractography using DT-MRI data. Magn Reson Imaging Med 2000; 44: 625–32.

Baylis GC, Rolls ET. Responses of neurons in the inferior temporal cortex in short term and serial recognition memory tasks. Exp Brain Res 1987; 65: 614–22.

Bechara A, Damasio AR, Damasio H, Anderson SW. Insensitivity to future consequences following damage to human prefrontal cortex. Cognition 1994; 50: 7–15.

Benson DA, Hienz RD, Goldstein MH Jr. Single-unit activity in the auditory cortex of monkeys actively localizing sound sources: spatial tuning and behavioral dependency. Brain Res 1981; 219: 249–67.

Brown JW, editor. Agnosia and apraxia: selected papers of Liepmann, Lange, and Pötzl. Translations by George Dean, Ellen Perecman, Emil Franzen, Joachim Luwisch. Hillside, NJ: Lawrence Erlbaum Associates; 1988.

Browning PG, Easton A, Gaffan D. Frontal-temporal disconnection abolishes object discrimination learning set in macaque monkeys. Cereb Cortex 2006 May 17; [Epub ahead of print].

Burdach KF. Vom Baue und Laben des Gehirns. Leipzig: in der Dyk'schen Buchhandlung; 1822–6.

Butter CM, Snyder DR, McDonald JA. Effects of orbital frontal lesions on aversive and aggressive behaviors in rhesus monkeys. J Comp Physiol Psychol 1970; 72: 132–44.

Catani M, Howard RJ, Pajevic S, Jones DK. Virtual in vivo interactive dissection of white matter fasciculi in the human brain. Neuroimage 2002; 17: 77–94.

Catani M, Jones DK, Donato R, Ffytche DH. Occipito-temporal connections in the human brain. Brain 2003; 126: 2093–107.

Catani M, Jones DK, Ffytche DH. Perisylvian language networks of the human brain. Ann Neurol 2005; 57: 8–16.

Ciccarelli O, Parker GJ, Toosy AT, Wheeler-Kingshott CA, Barker GJ, Boulby PA, et al. From diffusion tractography to quantitative white matter tract measures: a reproducibility study. Neuroimage 2003; 18: 348–59.

Clarke S, Thiran AB. Auditory neglect: what and where in auditory space. Cortex 2004; 40: 291–300.

Clarke S, Thiran AB, Maeder P, Adriani M, Vernet O, Regli L, et al. What and where in human audition: selective deficits following focal hemispheric lesions. Exp Brain Res 2002; 147: 8–15.

Cosgrove GR, Rauch SL. Stereotactic cingulotomy. Neurosurg Clin N Am 2003; 14: 225–35.

Cowan WM, Gottlieb DI, Hendrickson AE, Price JL, Woolsey TA. The autoradiographic demonstration of axonal connections in the central nervous system. Brain Res 1972; 37: 21–51.

Crosby EC, Schnitzlein HN. Comparative correlative neuroanatomy of the vertebrate telencephalon. New York: Macmillan; 1982.

Curran EJ. A new association fiber tract in the cerebrum with remarks on the fiber tract dissection method of studying the brain. J Comp Neurol Psychiat 1909; 19: 645–56.

Davis LE. An anatomic study of the inferior longitudinal fasciculus. Arch Neurol Psychiat 1921; 5: 370–81.

Dejerine JJ. Contribution à l'étude anatomo-pathologique et clinique des différentes variétés de cécité verbale. Mém Soc Biol 1892; 4: 61–90.

Dejerine JJ. Anatomie des centres nerveux. Paris: Rueff et Cie; 1895.

Denny-Brown D, Meyer JS, Horenstein S. The significance of perceptual rivalry resulting from parietal lesion. Brain 1952; 75: 433–71.

Devinsky O, Morrell MJ, Vogt BA. Contributions of anterior cingulate cortex to behaviour. Brain 1995; 118: 279–306.

Easton A, Ridley RM, Baker HF, Gaffan D. Unilateral lesions of the cholinergic basal forebrain and fornix in one hemisphere and inferior temporal cortex in the opposite hemisphere produce severe learning impairments in rhesus monkeys. Cereb Cortex 2002; 12: 729–36.

Ettinger AB. Commentary on personality changes following temporal lobectomy for epilepsy. Epilepsy Behav 2004; 5: 601–2.

Ferrari PF, Gallese V, Rizzolatti G, Fogassi L. Mirror neurons responding to the observation of ingestive and communicative mouth actions in the monkey ventral premotor cortex. Eur J Neurosci 2003; 17: 1703–14.

Filley CM. The behavioral neurology of white matter. New York: Oxford University Press; 2001.

Freeman W, Watts J. Psychosurgery: intelligence, emotion and social behavior following prefrontal lobotomy for mental disorders. Springfield: Charles C. Thomas; 1942.

Frey S, Kostopoulos P, Petrides M. Orbitofrontal involvement in the processing of unpleasant auditory information. Eur J Neurosci 2000; 12: 3709–12.

Gaffan D, Hornak J. Visual neglect in the monkey. Representation and disconnection. Brain 1997; 120: 1647–57.

Gaffan D, Parker A, Easton A. Dense amnesia in the monkey after transection of fornix, amygdala and anterior temporal stem. Neuropsychologia 2001; 39: 51–70.

Galletti C, Gamberini M, Kutz DF, Fattori P, Luppino G, Matelli M. The cortical connections of area V6: an occipito-parietal network processing visual information. Eur J Neurosci 2001; 13: 1572–88.

Geschwind N. Disconnexion syndromes in animals and man. Brain 1965; 88: 237–94.

Glaser GH. Treatment of intractable temporal lobe-limbic epilepsy (complex partial seizures) by temporal lobectomy. Ann Neurol 1980; 8: 455–9.

Goldberg ME, Segraves MA. Visuospatial and motor attention in the monkey. Neuropsychologia 1987; 25: 107–18.

Groswasser Z, Korn C, Groswasser-Reider I, Solzi P. Mutism associated with buccofacial apraxia and bihemispheric lesions. Brain Lang 1988; 34: 157–68.

Gunning-Dixon FM, Raz N. The cognitive correlates of white matter abnormalities in normal aging: a quantitative review. Neuropsychology 2000; 14: 224–32.

Heilman KM, Pandya DN, Geschwind N. Trimodal inattention following parietal lobe ablations. Trans Am Neurol Assoc 1970; 95: 259–61.

Heimer L. The human brain and spinal cord: functional neuronanatomy and dissection guide. 2n edn. New York: Springer-Verlag; 1995.

Helmstaedter C, Kurthen M, Lux S, Reuber M, Elger CE. Chronic epilepsy and cognition: a longitudinal study in temporal lobe epilepsy. Ann Neurol 2003; 54: 425–32.

Highley JR, Walker MA, Esiri MM, Crow TK, Harrison PJ. Asymmetry of the uncinate fasciculus: a post-mortem study of normal subjects and patients with schizophrenia. Cerebral Cortex 2002; 12: 1218–24.

Hill D, Pond DA, Mitchell W, Falconer MA. Personality changes following temporal lobectomy for epilepsy. J Mental Science 1957; 103: 18–27. Reprinted as Classics in Epilepsy and Behavior: 1957, in Epilepsy Behav 2004; 5: 603–10.

Kellenbach ML, Hovius M, Patterson K. A pet study of visual and semantic knowledge about objects. Cortex 2005; 41: 121–32.

Kubicki M, Westin C-F, Maier SE, et al. Uncinate fasciculus findings in schizophrenia: a magnetic resonance diffusion tensor imaging study. Am J Psychiatry 2002; 159: 813–20.

Leinonen L, Hyvarinen J, Sovijarvi AR. Functional properties of neurons in the temporo-parietal association cortex of awake monkey. Exp Brain Res 1980; 39: 203–15.

Levine B, Black SE, Cabeza R, et al. Episodic memory and the self in a case of isolated retrograde amnesia. Brain 1998; 121: 1951–73.

Levine B, Katz DI, Dade L, Black SE. Novel approaches to the assessment of frontal damage and executive deficits in traumatic brain injury. In: Stuss DT, Knight RT, editors. Principles of frontal lobe function. Oxford: Oxford University Press; 2002. p. 448–65.

Lichtheim L. On aphasia. Brain 1885; 7: 433–84.

Liepmann H, Maas O. Fall von linksseitiger Agraphie und Apraxie bei rechtsseitiger Lähmung. J Psychol Neurol 1907; 10: 214–27.

Ludwig E, Klingler J. Atlas cerebri humani. The inner structure of the brain demonstrated on the basis of macroscopical preparations. Boston: Little Brown; 1956.

MacLean PD. Some psychiatric implications of physiological studies on frontotemporal portion of limbic system (visceral brain). Electroencephalogr Clin Neurophysiol Suppl 1952; 4: 407–18.

Maeshima S, Truman G, Smith DS, Dohi N, Itakura T, Komai N. Buccofacial apraxia and left cerebral haemorrhage. Brain Inj 1997; 11: 777–82.

Makris N, Kennedy DN, McInerney S, Sorensen AG, Wang R, Caviness VS Jr, et al. Segmentation of subcomponents within the superior longitudinal fascicle in humans: a quantitative, in vivo, DT-MRI study. Cereb Cortex 2005; 15: 854–69.

Makris N, Worth AJ, Sorensen AG, Papadimitriou GM, Wu O, Reese TG, et al. Morphometry of in vivo human white matter association pathways with diffusion-weighted magnetic resonance imaging. Ann Neurol 1997; 42: 951–62.

Martinkauppi S, Rama P, Aronen HJ, Korvenoja A, Carlson S. Working memory of auditory localization. Cereb Cortex 2000; 10: 889–98.

Mesulam MM. A cortical network for directed attention and unilateral neglect. Ann Neurol 1981; 10: 309–25.

Meynert T. Psychiatry. A clinical treatise on diseases of the forebrain based upon a study of its structure, functions and nutrition. Part 1. The anatomy, physiology, and chemistry of the brain. Translated by B. Sachs. New York: G.P. Putnams' Sons; 1885.

Mishkin M. A memory system in the monkey. Phil Trans R Soc Lond series B 1982; 298: 85–95.

Moniz E. Prefrontal leucotomy in the treatment of mental disorders. J Psychiatry 1937; 93: 1379–85.

Mori S, van Zijl PC. Fiber tracking: principles and strategies – a technical review. NMR Biomed 2002; 15: 468–80.

Nakaji P, Meltzer HS, Singel SA, Alksne JF. Improvement of aggressive and antisocial behavior after resection of temporal lobe tumors. Pediatrics 2003; 112: e430.

O'Donnell LJ, Kubicki M, Shenton ME, Dreusicke MH, Grimson WE, Westin CF. A method for clustering white matter fiber tracts. Am J Neuroradiol 2006; 27: 1032–6.

Onufrowicz W. Das balkenlose Mikrocephalengehirn Hoffman. Ein Beitrag zur pathologischen und normalen Anatomie des menschlichen Gehirnes. Arch Psychiatrie 1887; 18: 305–28.

Peters A. The effects of normal aging on myelin and nerve fibers: a review. J Neurocytol 2002; 31: 581–93.

Peters A, Leahu D, Moss MB, McNally KJ. The effects of aging on area 46 of the frontal cortex of the rhesus monkey. Cereb Cortex 1994; 4: 621–35.

Petrides M. Impairments on nonspatial self-ordered and externally ordered working memory tasks after lesions of the mid-dorsal part of the lateral frontal cortex in the monkey. J Neurosci 1995; 15: 359–75.

Petrides M, Pandya DN. Projections to the frontal cortex from the posterior parietal region in the rhesus monkey. J Comp Neurol 1984; 228: 105–116.

Petrides M, Pandya DN. Association fiber pathways to the frontal cortex from the superior temporal region in the rhesus monkey. J Comp Neurol 1988; 273: 52–66.

Petrides M, Pandya DN. Efferent association pathways originating in the caudal prefrontal cortex in the macaque monkey. J Comp Neurol 2006; 498: 227–51.

Pressman JD. Sufficient promise: John F. Fulton and the origins of psychosurgery. Bull Hist Med 1988; 62: 1–22.

Preuss TM, Goldman-Rakic PS. Connections of the ventral granular frontal cortex of macaques with perisylvian premotor and somatosensory areas: anatomical evidence for somatic representation in primate frontal association cortex. J Comp Neurol 1989; 282: 293–316.

Rasmussen T. Surgical aspects of temporal lobe epilepsy. Results and problems. Acta Neurochir Suppl (Wien) 1980; 30: 13–24.

Rauschecker JP, Tian B. Mechanisms and streams for processing of "what" and "where" in auditory cortex. Proc Natl Acad Sci USA 2000; 97: 11800–6.

Rauschecker JP, Tian B, Hauser M. Processing of complex sounds in the macaque nonprimary auditory cortex. Science 1995; 268: 111–4.

Reil JC. Die Sylvische Grube oder das Thal, das gestreifte grosse Hirnganglium, dessen Kapsel und die Seitentheile des grossen Gehirns. Archiv für die Physiologie. Halle, Curtschen Buchhandlung 1809; 9: 195–208.

Rizzolatti G, Fadiga L, Fogassi L, Gallese V. Resonance behaviors and mirror neurons. Arch Ital Biol 1999; 137: 85–100.

Rizzolatti G, Matelli M. Two different streams form the dorsal visual system: anatomy and functions. Exp Brain Res 2003; 153: 146–57.

Rizzolatti G, Matelli M, Pavesi G. Deficits in attention and movement following the removal of postarcuate (area 6) and prearcuate (area 8) cortex in macaque monkeys. Brain 1983; 106: 655–73.

Schiff HB, Alexander MP, Naeser MA, Galaburda AM. Aphemia. Clinical-anatomic correlations. Arch Neurol 1983; 40: 720–7.

Schmahmann JD, Pandya DN. Fiber pathways of the brain. New York: Oxford University Press; 2006.

Schröder P. Das fronto-occipitale Associationsbündel. Ein kritischer Beitrag. Monatsschr Psychiatrie Neurol 1901; 9: 81–99.

Selden NR, Gitelman DR, Salamon-Murayama N, Parrish TB, Mesulam MM. Trajectories of cholinergic pathways within the cerebral hemispheres of the human brain. Brain 1998; 121: 2249–57.

Seltzer B, Pandya DN. Further observations on parieto-temporal connections in the rhesus monkey. Exp Brain Res 1984; 55: 301–12.

Spangler WJ, Cosgrove GR, Ballantine HT, Cassem EH, Rauch SL, Nierenberg A, et al. Magnetic resonance image-guided stereotactic cingulotomy for intractable psychiatric disease. Neurosurgery 1996; 38: 1071–8.

Spiegler BJ, Mishkin M. Evidence for the sequential participation of inferior temporal cortex and amygdala in the acquisition of stimulus-reward associations. Behav Brain Res 1981; 3: 303–17.

Squire LR, Zola-Morgan S. The medial temporal lobe memory system. Science 1991; 253: 1380–6.

Stuss DT, Benson DF. The frontal lobes. New York: Raven Press; 1986.

Suzuki H, Azuma M. Prefrontal unit activity during gazing at a light spot in the monkey. Brain Res 1977; 126: 497–508.

Taoka T, Iwasaki S, Sakamoto M, et al. Diffusion anisotropy and diffusivity of white matter tracts within the temporal stem in Alzheimer disease: evaluation of the "tract of interest" by diffusion tensor tractography. Am J Neuroradiol 2006; 27: 1040–5.

Tench CR, Morgan PS, Wilson M, Blumhardt LD. White matter mapping using diffusion tensor MRI. Magn Reson Med 2002; 47: 967–72.

Trolard P. Le faisceau longitudinal inférieur du cerveau. Rev Neurol 1906; 14: 440–46.

Tsao DY, Freiwald WA, Knutsen TA, Mandeville JB, Tootell RB. Faces and objects in macaque cerebral cortex. Nat Neurosci 2003; 6: 989–95.

Tuch DS, Reese TG, Wiegell MR, Makris N, Belliveau JW, Wedeen VJ. High angular resolution diffusion imaging reveals intravoxel white matter fiber heterogeneity. Magn Reson Med 2002; 48: 577–82.

Ungerleider LG, Mishkin M. Two cortical visual systems. In: Ingle DJ, Goodale MA, Mansfield RJW, editors. Analysis of visual behavior. Cambridge, MA: MIT Press; 1982. p. 549–86.

Wedeen VJ, Hagmann P, Tseng WY, Reese TG, Weisskoff RM. Mapping complex tissue architecture with diffusion spectrum magnetic resonance imaging. Magn Reson Med 2005; 54: 1377–86.

Wernicke C. Der aphasische Symptomencomplex. Eine psychologische Studie auf anatomischer Basis. Cohn: Breslau; 1874.

Winterer G, Coppola R, Egan MF, Goldberg TE, Weinberger DR. Functional and effective frontotemporal connectivity and genetic risk for schizophrenia. Biol Psychiatry 2003; 54: 1181–92.

Wise RJ, Scott SK, Blank SC, Mummery CJ, Murphy K, Warburton EA. Separate neural subsystems within 'Wernicke's area'. Brain 2001; 124: 83–95.

Woolley JD. Buccofacial apraxia and the expression of emotion. Ann NY Acad Sci 2003; 1000: 395–401.